Title: Arc1 modulates microbiota-responsive developmental and metabolic traits in *Drosophila*

Running Title: Arc1 and *Acetobacter* promote fly growth

Keywords: *Drosophila*, microbiota, *Acetobacter*, Arc1, insulin signaling, metabolism

Scott A. Keith*, Cassandra Bishop*†, Samantha Fallacaro*†, Brooke M. McCartney*

* Department of Biological Sciences, Carnegie Mellon University, Pittsburgh, PA 15213

† Equal contribution

Corresponding author:

Brooke M. McCartney

600D Mellon Institute

Department of Biological Sciences

Carnegie Mellon University

4400 Fifth Avenue

Pittsburgh, PA 15213

Phone: (412) 268-5195

Email: bmccartney@cmu.edu

SUMMARY

Drosophila Arc1 exhibits microbiota-dependent, tissue-specific differential expression, mitigates the impacts of germ-free rearing on insulin signaling and growth rate, but is dispensable for metabolic homeostasis in *Acetobacter*-colonized flies.

ABSTRACT

Perturbations to animal-associated microbial communities (the microbiota) have deleterious effects on various aspects of host fitness, including dysregulated energy metabolism. However, the molecular processes underlying these microbial impacts on the host are poorly understood. In this study, we identify a novel connection between the microbiota and the neuronal factor Arc1 that affects metabolism and development in *Drosophila*. We find that *Arc1* exhibits tissue-specific microbiota-dependent expression changes, and that flies bearing a null mutation of *Arc1* complete larval development at a dramatically slowed rate compared to wild-type animals. In contrast, monoassociation with a single *Acetobacter sp.* isolate was sufficient to enable *Arc1* mutants to develop at a wild-type rate. These developmental phenotypes are highly sensitive to composition of the larval diet, suggesting the growth rate defects of GF flies lacking Arc1 reflect metabolic dysregulation. Additionally, we show that pre-conditioning the larval diet with *Acetobacter sp.* partially accelerates *Arc1* mutant development, but live bacteria are required for the full growth rate promoting effect. Finally, GF *Arc1* mutants display multiple traits consistent with reduced insulin signaling activity that are reverted by association with *Acetobacter sp.*, suggesting a potential mechanism underlying the microbe-dependent developmental phenotypes. Our results reveal a novel role for Arc1 in modulating insulin

signaling, metabolic homeostasis, and growth rate that is specific to the host's microbial and nutritional environment.

INTRODUCTION

The physiology and life history traits of animals are shaped in remarkable ways by interactions with commensal and beneficial microorganisms (the microbiota). For many metazoans, microbial symbionts play integral roles in post-embryonic development and physiology to yield fit and fertile adults (McFall-Ngai et al., 2013; Robertson et al., 2019). Thus, perturbations to the microbiota can have profoundly deleterious consequences for its animal host. For example, germ free (GF) or antibiotic-treated mice exhibit decreased body fat (Smith et al., 2007), abnormal intestinal epithelial architecture (Hayes et al., 2018), fewer differentiated immune cells (Ekmekciu et al., 2017), and neurodevelopmental defects (Sampson and Mazmanian, 2015). In humans, dysbiosis of the gut microbiota has been implicated in the pathogenesis of a wide range of disorders, such as Type 2 diabetes (Larsen et al., 2010), obesity (Shen et al., 2013), and autism (Gilbert et al., 2013). However, the molecular factors that actuate microbial influence on host physiology and development are not comprehensively understood. *Drosophila melanogaster* and its gut microbiota are an ideal model to discover such factors given *Drosophila*'s extensive genetic resources, the low-diversity and readily-cultured bacterial communities associated with laboratory fly cultures, and the consequent technical ease of generating GF and gnotobiotic fly populations (Broderick and Lemaitre, 2012; Douglas, 2018; Martino et al., 2017).

From a screen to discover microbiota-responsive neuronal genes, we identified *Drosophila Activity-regulated cytoskeleton associated protein 1* (*Arc1*) as being

differentially expressed in GF flies. *Arc1* is a *Drosophila* homolog of mammalian Arc/Arg3.1, an immediate early gene and master regulator of synaptic plasticity in the brain (Carmichael and Henley, 2018; Shepherd and Bear, 2011). Arc transcription is highly upregulated by synaptic activity and while the brain is encoding novel information into neural circuits (Chen et al., 2020; Guzowski et al., 1999). Accordingly, reduced Arc expression impairs memory formation and learning ability in rodents (Guzowski et al., 2000; Shandilya and Gautam, 2020), and defects in human Arc function have been linked to a variety of neurological and neurodevelopmental disorders, including Alzheimer's disease (Bi et al., 2018), autism spectrum disorders (Alhowikan, 2016), and schizophrenia (Fromer et al., 2014). Arc partially regulates synaptic plasticity by interacting with endocytic machinery to regulate synaptic surface presentation of AMPA-type glutamate receptors (Chowdhury et al., 2006; DaSilva et al., 2016; Wall and Corrêa, 2018). Both mammalian *Arc* and fly *Arc1* encode retroviral group-specific antigen-like amino acid sequences, and are predicted to have independently derived from ancient Ty3/Gypsy retrotransposons (Ashley et al., 2018; Campillos et al., 2006; Cottee et al., 2019; Pastuzyn et al., 2018). Recently, it was shown that Arc and Arc1 proteins can self-assemble into capsid-like structures that package and transport mRNAs (including *Arc*/*Arc1* mRNA) into cultured neuronal cell lines and across synapses *in vivo*, constituting a novel mechanism of cell-cell communication (Ashley et al., 2018; Erlendsson et al., 2019; Pastuzyn et al., 2018).

As with mammalian *Arc*, *Drosophila Arc1* expression is strongly upregulated by neuronal activation (Guan et al., 2005; Mattaliano et al., 2007; Montana and Littleton, 2006; Mosher et al., 2015). At the larval neuromuscular junction (NMJ), Arc1 protein-

93 mediated transfer of *Arc1* mRNA from the boutons of motoneurons to post-synaptic
94 myocytes appears to be required for appropriate synapse maturation and synaptic
95 plasticity (Ashley et al., 2018). Further, *Arc1* loss-of-function mutants have elevated fat
96 levels, altered metabolomic profiles, are starvation resistant, and differentially express a
97 repertoire of enzymes involved in central carbon metabolism (Mattaliano et al., 2007;
98 Mosher et al., 2015). These phenotypes may be at least partially attributable to Arc1
99 activity in the brain, where its expression in adults is concentrated in a subset of large
100 neurons in the pars intercerebralis (Mattaliano et al., 2007). However, the precise cellular
101 pathways and mechanisms through which it affects metabolism are not known.

102 In *Drosophila,* metabolic functions directly impact developmental timing and whole-
103 organism growth that occurs exclusively during the larval stages (Edgar, 2006). Fly larvae
104 progress through three developmental instars, increasing in size approximately 200-fold
105 prior to pupariation and metamorphosis (Robertson, 1963). Both the timing of
106 developmental progression and the magnitude of larval growth are genetically regulated
107 by multiple intersecting nutrient-responsive inter-organ signaling pathways, including the
108 insulin/insulin-like growth factor (IIS) pathway (Brogiolo et al., 2001; Rulifson et al., 2002),
109 the 20-hydroxyecdysone biosynthetic pathway (Buhler et al., 2018; McBrayer et al.,
110 2007), and target-of-rapamycin (TOR) signaling (Colombani et al., 2003; Layalle et al.,
111 2008). IIS and TOR signaling are highly functionally conserved between *Drosophila* and
112 vertebrates (Edgar, 2006; Gilbert, 2008). The microbiota also has a significant impact on
113 fly metabolism; GF larvae exhibit prolonged larval development and stunted growth
114 compared to conventionally-reared or gnotobiotic flies (Newell and Douglas, 2014; Shin
115 et al., 2011; Storelli et al., 2011; Storelli et al., 2017; Wong et al., 2014). Commensal

116 bacteria appear to impact Drosophila growth through numerous mechanisms, including
117 nutritional provisioning and activation of host signaling pathways via secreted metabolites
118 (Chaston et al., 2014; Consuegra et al., 2020; Kamareddine et al., 2018; Keebaugh et al.,
119 2018; Matos et al., 2017; Sannino et al., 2018; Shin et al., 2011). However, many gaps
120 remain in our understanding of the molecular mechanisms linking the bacterial microbiota
121 to larval metabolic function and growth dynamics.

122 Here we reveal *Arc1* as a novel host factor that modulates the microbiota's impact
123 on larval growth. *Arc1* is transcriptionally altered in tissue-specific patterns in GF flies,
124 and loss of *Arc1* dramatically exacerbates the developmental growth delay of GF larvae.
125 We further show that a single *Acetobacter* isolate is sufficient to restore normal larval
126 development in *Arc1* mutants, and that pre-conditioning the larval diet with this
127 *Acetobacter sp.* partly restores a normal growth rate to GF *Arc1* mutants. We further show
128 that loss of both *Arc1* and the microbiota results in multiple traits consistent with reduced
129 insulin/insulin-like growth factor (IIS) pathway activity, and that monoassociation with
130 *Acetobacter sp.* reduces the severity of these phenotypes. Together our data reveal an
131 experimental system wherein a single microbiota member supports the health of a
132 metabolically destabilized host genotype. Further, this work demonstrates a previously
133 unrecognized role for *Arc1* in altering insulin signaling in flies following microbiota
134 removal.

135 **RESULTS**

136 **The microbiota promote larval development of *Arc1*-deficient *Drosophila* hosts**

137 To identify host neuronal molecules and pathways that may be impacted by the
138 microbiota, we conducted a transcriptomic screen to identify *Drosophila* genes that are

139 differentially expressed in adult fly heads upon elimination of the bacterial microbiota.
140 From this work, we identified *Arc1* among the genes that were most responsive to host
141 microbial condition (Keith et al., 2019, bioRxiv). Specifically, we found that *Arc1*
142 transcripts are elevated in the heads of adult wild-type *Drosophila* grown under germ-free
143 conditions (GF; microbiologically sterile) compared to flies grown in gnotobiotic (GNO)
144 polyassociation with a four-species bacterial community consisting of two *Acetobacter*
145 (*Acetobacter sp.*, *A. pasteurianus*) and two *Lactobacillus* (*L. brevis*, *L. plantarum*) isolates
146 (Figure 1A). Notably, in published RNA-seq datasets comparing the gut transcriptomes
147 of microbiota-associated *Drosophila* to GF guts, *Arc1* is among the significantly
148 differentially expressed genes (Bost et al., 2017; Dobson et al., 2016; Guo et al., 2014;
149 Petkau et al., 2017); consistent with these studies, we found that *Arc1* is transcriptionally
150 decreased in the adult GF gut (Figure 1A). These microbiota-sensitive transcript level
151 changes occur in multiple wild-type fly lines, but both changes were not observed in every
152 wild type line (Figure 1A). Together our data demonstrate that *Arc1* is a microbiota-
153 responsive gene, and the transcript response exhibits tissue specificity.

154 *Arc1* regulates lipid homeostasis and central carbon metabolite levels in
155 *Drosophila* larvae (Mosher et al., 2015), and an *Arc1* loss of function mutant exhibits
156 enhanced starvation resistance in adult flies (Mattaliano et al., 2007). Intriguingly, recent
157 studies have shown that these and other metabolic traits are also impacted by the
158 microbiota, depending on dietary conditions and host genetic background (reviewed in
159 Douglas, 2018). One of the major organism-level consequences of GF-induced metabolic
160 dysregulation in *Drosophila* is a prolonged larval growth period (Strigini and Leulier,
161 2016). Thus, to test for a physiologically relevant interaction between the microbiota and

162 *Arc1* function, we raised wild-type flies (w^{1118}) and a fly line bearing a CRISPR-mediated
163 deletion of *Arc1* ($Arc1^{E8}$; Ashley et al., 2018) from embryo to adulthood either GF or GNO,
164 and monitored their larval growth rate. Consistent with many previous reports (Chaston
165 et al., 2014; Consuegra et al., 2020; Erkosar et al., 2015; Kamareddine et al., 2018;
166 Keebaugh et al., 2018; Newell and Douglas, 2014; Sannino et al., 2018; Shin et al., 2011;
167 Storelli et al., 2011; Storelli et al., 2017; Wong et al., 2014), we found that GNO wild-type
168 animals completed larval development faster than their GF siblings (Figure 1B). On our
169 laboratory's routine diet (see Material and Methods) at 23ºC, wild-type GNO cultures take
170 ~7 days to complete larval development, and this period is extended by ~1.5 days under
171 GF conditions (Figure 1B, Table S1). Strikingly, the larval growth delay induced by
172 microbiota elimination was dramatically extended in larvae lacking *Arc1*. While $Arc1^{E8}$
173 mutant larvae grown under GNO conditions developed at a rate indistinguishable from
174 wild-type GNO larvae, GF $Arc1^{E8}$ animals took on average ~12 days to complete larval
175 development (Figure 1B). These differences in larval growth rate were reflected in the
176 rate of adult emergence, with wild-type and $Arc1^{E8}$ GNO animals eclosing ~12.5 days
177 after embryo deposition, wild-type GF eclosing after ~14 days, and $Arc1^{E8}$ GF adults
178 emerging asynchronously between 16-20 days (Figure S1A). We observed a similar,
179 though less protracted, developmental delay for two independently-generated *Arc1* loss-
180 of-function alleles ($Arc1^{esm18}$ and $Arc1^{esm113}$; Mattaliano et al., 2007) under GF conditions
181 (Figures S1B, C), and in GF animals transheterozygous for $Arc1^{E8}$ and $Arc1^{esm113}$ (Figure
182 1C). Further, ablation of *Arc1*-expressing cells using *Arc1-GAL4* (Mattaliano et al., 2007)
183 to drive expression of the pro-apoptotic *reaper* also extended the developmental period
184 of GF larvae (Figure 1D). All larvae bearing loss of function mutations in *Arc1* or ablation

185 of *Arc1* expressing cells developed at the wild type rate when grown with the GNO
186 bacterial community. *Arc2* is another *Drosophila* Arc homolog in a genomic locus adjacent
187 to *Arc1*; the two proteins likely represent an ancestral duplication event (Pastuzyn et al.,
188 2018). In contrast to *Arc1* depletion, a P-element insertion in the *Arc2* 3' UTR which
189 decreased *Arc2* expression (Figure S1D) had no effect on the developmental rate of GF
190 larvae (Figure S1E). Together these results suggest a reciprocal host gene-microbe
191 interaction: the bacterial microbiota facilitates the appropriate larval growth rate of *Arc1*-
192 deficient larvae, and Arc1 is a novel host protein that modulates the physiological
193 response to microbiota loss during larval development.

194 **Monoassociation with *Acetobacter sp.* is sufficient to promote larval development**
195 **of *Arc1* mutant larvae**

196 We next asked whether the ability of our polymicrobial GNO community to promote
197 larval growth rate was attributable to the effects of individual bacterial taxa or collective
198 effects of the community. To this end, we generated wild-type and *Arc1* null fly cultures
199 in monoassociation with each of the four bacteria and measured time to complete larval
200 development. Wild-type larvae monoassociated with each of the four bacteria developed
201 significantly faster than their GF siblings, with the two *Acetobacter* isolates promoting
202 slightly faster development than the two *Lactobacillus* isolates (Figure 2A). In contrast,
203 only $Arc1^{E8}$ mutant larvae monoassociated with *Acetobacter sp.* developed at an identical
204 rate to polyassociated GNO larvae; *Arc1* mutants associated with *A. pasteurianus*, *L.*
205 *brevis*, and *L. plantarum* all developed at the same rate, ~2 days faster than GF, but ~2.5-
206 3 days slower than GNO and *Acetobacter sp.* monoassociated larvae (Figure 2B). While
207 we did find significant differences in bacterial load among the four isolates, these

208 differences did not correlate with the impact of each bacteria on host developmental rate
209 for either genotype (Figure S2).

210 Because *Acetobacter sp.* alone was sufficient to enable *Arc1*^{E8} larvae to achieve
211 a wild-type growth rate, we asked whether it would also be necessary in the four-species
212 GNO community. Surprisingly, while mutant larvae associated with *A. pasteurianus*, *L.*
213 *brevis*, and *L. plantarum* alone developed substantially slower than those associated with
214 the four-species group or *Acetobacter sp.*, the three together in a GNO community lacking
215 *Acetobacter sp.* were sufficient to promote normal development. However, for
216 experimental tractability we focused all subsequent investigation on wild type and *Arc1*
217 mutants monoassociated with *Acetobacter sp.*.

218 While the delayed pupariation rate of wild-type GF larvae reflects a moderately
219 extended duration of all three larval instars (Figure 2C; Storelli et al., 2011), *Arc1*^{E8} GF
220 larvae undergo substantially prolonged L1 and L2 phases (Figure 2C). Further, GF
221 animals of both genotypes increase in size at a more gradual rate than those with
222 *Acetobacter sp.*, but this effect is highly exaggerated in *Arc1* mutants, suggesting a longer
223 time to attain the critical weights that trigger each molt and metamorphosis (Figure 2D;
224 Mirth et al., 2005). The extended larval period could reflect reduced food consumption,
225 but we did not observe feeding differences in *Arc1*-deficient larvae under either microbial
226 condition (Figure S3). Along with a lengthened time to pupariation, both wild-type and
227 *Arc1*^{E8} GF larvae develop into smaller pupae, but, as with the developmental delay, this
228 size reduction is greater for animals lacking *Arc1* (Figure 2E). These data suggest that
229 loss of *Arc1* exacerbates the effects of GF rearing on both larval growth rate and growth
230 capacity.

231 **Host diet can modulate the *Arc1*-dependent GF larval developmental delay**

232 The developmental rate of wild type GF larvae is particularly sensitive to the
233 concentration of dietary yeast, the primary source of ingested amino acids: the
234 developmental lag of GF compared to conventional (CV) or GNO animals increases on
235 diets with low yeast content, while feeding high-yeast diets enables GF larvae to develop
236 at the same rate as microbe-associated larvae (Shin et al., 2011; Storelli et al., 2011;
237 Wong et al., 2014). To determine how the loss of Arc1 impacts the dietary sensitivity of
238 GF larvae, we reared *Acetobacter sp.*-associated and GF wild-type and $Arc1^{E8}$ larvae on
239 nine simplified diets containing systematically varied concentrations of dextrose and
240 yeast, and monitored time to pupariation (Figure 3).

241 As expected, in wild-type animals "high-yeast" (10%) diets eliminated the
242 developmental gap between *Acetobacter sp.*-associated and GF larvae, regardless of
243 glucose concentration, while on "low-yeast" (3%) diets wild-type GF larvae were
244 consistently delayed. The exception to this was the 3% yeast-10% glucose diet, which
245 substantially slowed the developmental rate of all conditions, a known effect of high-
246 sugar, low-protein diets (Musselman et al., 2011; Wong et al., 2014). Interestingly, on 5%
247 yeast diets, increasing glucose concentration moderately accelerated the development of
248 wild-type GF larvae, with a statistically significant delay observed only at the lowest
249 glucose level. Overall, these data are congruent with published observations that GF
250 rearing predominantly sensitizes wild-type flies to reductions in dietary protein content.

251 GF larvae lacking *Arc1* generally showed enhanced developmental sensitivity to
252 dietary composition; GF $Arc1^{E8}$ animals developed more slowly than GF wild-type on five
253 out of the nine tested diets (Figure 3). Notably, GF $Arc1^{E8}$ larvae were even delayed on

254 two “high-yeast” diets (10% yeast-3% glucose and 10%yeast-10% glucose), where the
255 wild type GF larvae developed at same rate as wild type *Acetobacter sp.* animals. On
256 most diets, *Arc1* mutants associated with *Acetobacter sp.* developed at the same rate as
257 wild-type *Acetobacter sp.*-associated larvae. One notable exception was the 3% yeast-
258 5% glucose diet, where *Acetobacter sp.* failed to have any growth rate promoting activity
259 for $Arc1^{E8}$ larvae.

260 Importantly, while *Arc1*-deficient larvae grown GF still displayed a lengthened
261 duration of larval development on multiple diets, none of the tested formulations yielded
262 a magnitude of delay comparable to that observed on our laboratory’s routine diet (Figure
263 1B). To compare the nutritional contents of the yeast-glucose diets to our cornmeal-yeast-
264 molasses diet (see Materials and Methods), we utilized the *Drosophila* Dietary
265 Composition Calculator to determine the protein:carbohydrate (P:C) ratio of each recipe
266 (Figure 3; Lesperance and Broderick, 2020). Relative to most of the tested yeast-glucose
267 diets, our laboratory diet has a low P:C ratio of 0.06. Interestingly, the yeast-glucose diet
268 with the P:C ratio closest to that of our diet (3% yeast-10% glucose; P:C 0.09) did not
269 recapitulate the microbe-dependent developmental rate trends observed on our diet;
270 specifically, *Acetobacter sp.*-associated wild-type and *Arc1* mutant larvae developed
271 substantially slower on this yeast-glucose diet than on our diet. This may indicate that the
272 full growth rate promoting effects of this *Acetobacter sp.* are specific to the more complex
273 nutritional substrate of the cornmeal-yeast-molasses diet and less dependent on the
274 relative proportions of these two macronutrients. For example, cornmeal provides sugars
275 in the form of complex polysaccharides that require a multi-step breakdown process
276 involving amylases and maltases, which have previously been shown to be microbiota

277 responsive in *Drosophila* larvae (Erkosar et al., 2017). Additionally, differences in
278 *Acetobacter sp.* developmental support could be due to different levels of bacterial
279 population growth on the various diets.

280 Together, these results indicate that the importance of *Arc1* function during GF
281 larval development is highly dependent on the host's nutritional environment, and suggest
282 that *Arc1* may be particularly important for GF animals' metabolic responses to dietary
283 amino acid availability.

284 **Live *Acetobacter sp.* populations are required for optimal *Arc1* mutant**
285 **developmental rate**

286 We next sought to investigate the mechanisms by which *Acetobacter sp.*
287 association enables *Arc1*-deficient animals to complete larval development at the same
288 rate as wild-type monoassociated animals. Given that increasing the concentration of
289 dietary yeast can substantially diminish the prolonged larval stage of GF *Arc1* mutant
290 larvae, we hypothesized that bacteria consumed with the diet may serve as a
291 supplemental food source supporting $Arc1^{E8}$ development, a mechanism for which there
292 is precedent in wild-type *Drosophila* (Bing et al., 2018; Keebaugh et al., 2018; Storelli et
293 al., 2017). To test this prediction, we inoculated GF wild-type and $Arc1^{E8}$ cultures with
294 heat-killed *Acetobacter sp.* cells daily throughout the larval developmental period until the
295 entire population pupariated. Administration of heat-killed *Acetobacter* resulted in a slight,
296 but not statistically significant, acceleration of developmental rate for GF *Arc1* mutants
297 (Figure 4A). Feeding with dead *Acetobacter* cells had no effect on wild-type GF larval
298 developmental rate (Figure 4A). These data suggest *Acetobacter sp.* does not solely
299 serve as a nutritional supplement to promote *Arc1* mutant development.

300 The *Acetobacteraceae* are distinguished by the ability to generate acetic acid
301 through partial oxidation of ethanol and other substrates (Saichana et al., 2015). Two
302 studies showed that acetic acid/acetate consumption enables GF larvae or larvae
303 associated with an *Acetobacter* mutant deficient for acetic acid production to develop at
304 a rate comparable to those associated with live bacteria (Kamareddine et al., 2018; Shin
305 et al., 2011); in contrast, acetic acid has also been reported to yield no effect on growth
306 in a GF context, or, at higher concentrations, further extends the GF larval growth delay
307 (Kim et al., 2017; Shin et al., 2011). Consistent with the latter results, we found that
308 providing GF wild type or *Arc1*^{E8} larvae with dietary acetic acid at different concentrations
309 either had no impact on growth rate, or increased the duration of larval development
310 (Figure 4C, C'). This suggests that any acetic acid generation by our *Acetobacter sp.*
311 isolate has minimal impact on larval growth under our dietary and husbandry conditions.
312 We also found that daily inoculation with filtered supernatant from planktonic *Acetobacter*
313 *sp.* cultures had no effect on either wild-type or *Arc1*^{E8} GF larvae, providing no evidence
314 to support a role for metabolite(s) secreted in *Acetobacter sp.* planktonic culture in
315 promoting larval growth rate (Figure 4B).

316 The association of larval and adult *Drosophila* with their commensals involves
317 bacterial proliferation on the flies' diet and consequent continual ingestion of live and dead
318 bacterial cells associated with the food bolus (Ludington and Ja, 2020). The host and its
319 microbial partners therefore share a dietary niche, with the bacteria utilizing the flies' food
320 as a carbon source (Blum et al., 2013; Martino et al., 2018; Storelli et al., 2017). Prior
321 work suggests that certain microbe-affected metabolic traits in *Drosophila*, including
322 growth rate, result from bacterial utilization of dietary nutrients (Consuegra et al., 2020;

323 Huang and Douglas, 2015; Storelli et al., 2017). These microbiota-dependent host traits
324 therefore arise from bacterial modification of the flies' diet, resulting in an altered
325 nutritional intake. We hypothesized that bacterial dietary modification might underlie
326 *Acetobacter sp.* support of *Arc1* mutant development. To test this hypothesis, we
327 inoculated GF food vials with *Acetobacter sp.* planktonic culture, allowed colonization of
328 the diet for five days, and then heat-treated the vials to kill all bacteria, resulting in an
329 *Acetobacter sp.*-conditioned but microbiologically sterile larval food substrate.

330 When fed the conditioned diet, wild-type GF larvae also developed slightly, though
331 not significantly, faster than wild-type GF larvae on regular sterile food, and on un-
332 inoculated sterile food subjected to the same heat treatment used to sterilize conditioned
333 media (Figure 4D). In contrast, *Acetobacter sp.*-conditioned food substantially
334 accelerated GF $Arc1^{E8}$ larval development compared to GF larvae on untreated and
335 heated control diets, though still ~1.5 days slower than *Arc1* mutants associated with live
336 *Acetobacter sp.* (Figure 4D'). These data suggest that *Acetobacter sp.* modification of the
337 larval diet may be an important, though not exclusive, mechanism by which this bacterial
338 isolate promotes larval growth rate.

339 **Germ free rearing alters metabolic defects of *Arc1* mutant animals and reduces**
340 **insulin signaling**

341 The rate of larval growth and development in *Drosophila* is an organism-level
342 readout of systemic energy metabolism. Specifically, growth is promoted by the activation
343 of multiple circulating-hormone-regulated signaling pathways, including the
344 insulin/insulin-like signaling (IIS) pathway, which are responsive to and downstream of
345 nutrient intake (Edgar, 2006). Following food consumption, insulin-like peptides (Ilps) are

346 synthesized by neuroendocrine cells in the brain and released into the hemolymph
347 (Géminard et al., 2009). Ilps then circulate to principal metabolic tissues, including the fat
348 body, and activate the insulin receptor (InR; Brogiolo et al., 2001; DiAngelo and Birnbaum,
349 2009). This results in the nuclear exclusion of the transcription factor Foxo, the
350 suppression of starvation responses, and growth promotion (Jünger et al., 2003; Kramer
351 et al., 2003). Decreased IIS activity results in a larval growth delay, or in the most severe
352 cases a complete growth arrest (reviewed in Baker and Thummel, 2007). Furthermore, in
353 wild-type animals fed nutrient restrictive diets, individual commensal bacteria, including
354 some *Acetobacter*, may promote larval growth and development in part via activation of
355 host IIS (Kamareddine et al., 2018; Shin et al., 2011; Storelli et al., 2011). *Arc1* has been
356 previously implicated in metabolic homeostasis (Mosher et al., 2015), but not IIS signaling
357 (Mattaliano et al., 2007). Further, we have shown that the growth rate of GF *Arc1* mutants
358 is delayed and sensitive to dietary composition (Figure 3), consistent with metabolic
359 dysregulation. Thus, we hypothesized that the developmental delay of $Arc1^{E8}$ GF larvae
360 is a consequence of reduced IIS activity, and that *Acetobacter sp.* supports an appropriate
361 $Arc1^{E8}$ growth rate by restoring proper IIS signaling.

362 In addition to a reduction in larval growth rate, loss of IIS signaling results in other
363 growth defects. This includes a reduction in wing size, due to a reduction in cell number
364 and cell size (Figure 5A; Rulifson et al., 2002). While wild-type GF larvae have a
365 decreased larval growth rate (Figure 1B), and final larval size (Figure 2E), we did not
366 observe any alteration to wing growth properties: cell size (inferred by cell density), cell
367 number, and wing size were indistinguishable from that of *Acetobacter sp.*-associated

368 wild type animals (Fig. 5B-D). This may suggest that larval growth rate is particularly
369 sensitive to metabolic perturbations under our culture conditions.

370 *Arc1* mutants grown under GF conditions exhibited a significant reduction in cell
371 size, consistent with reduced IIS activity, whereas *Acetobacter sp.*-associated mutant
372 wings had wild-type sized cells (Figure 5A,B). Surprisingly, though, loss of Arc1 increased
373 cell number, regardless of microbial condition (Figure 5A,C). Since cell size was
374 unaffected in *Arc1*^{E8}*-Actobacter sp.* flies, this resulted in larger wings for these animals,
375 whereas GF *Arc1*^{E8} wings were the same size as wild-type wings, due to their reduced
376 cell size (Figure 5A,D). While increased IIS activity is associated with larger wings, this is
377 accompanied by an increase in cell size (Brogiolo et al., 2001). This suggests that Arc1
378 may also contribute to wing growth through unknown additional mechanisms.

379 In addition to growth changes, loss of IIS pathway activity also results in resistance
380 to adult starvation conditions (Broughton et al., 2005). *Arc1*^{esm18} mutants are likewise
381 starvation resistant (Mattaliano et al., 2007). We observed the same phenotype, with
382 *Arc1*^{E8} *Acetobacter sp.* females taking longer to succumb to starvation than wild type
383 *Acetobacter sp.* and wild type GF adults. This starvation resistance was strongly
384 enhanced in GF *Arc1*^{E8} animals, which survived full nutrient deprivation ~two days longer
385 than wild type animals (Figure 5E). Reduced mobilization of energy stores under
386 starvation conditions is another consequence of reduced IIS activity (Broughton et al.,
387 2005; Luong et al., 2006). Thus, the strongly enhanced starvation survival of GF *Arc1*
388 mutants, are consistent with deficient IIS function in the absence of *Arc1* and the
389 microbiota.

390 Activation of the insulin receptor (InR) results in the activation of PI3K increasing
391 the membrane phospholipid PIP_3 (Britton et al., 2002). This produces a membrane-
392 associated binding site for proteins containing the Plextrin homology (PH) domain,
393 including the IIS effector Akt (Verdu et al., 1999). tGPH is a GFP-tagged PH domain that
394 has been widely used as an *in vivo* reporter of PI3K activity and IIS pathway activation
395 (Britton et al., 2002). In *Acetobacter sp.*-associated wild-type and $Arc1^{E8}$ larvae and in
396 wild-type GF larvae, we observed a strong membrane localization of tGPH in the fat body
397 that was indistinguishable between those genotypes and conditions (Fig. 5F), suggesting
398 that IIS signaling is not significantly perturbed in these larvae. In contrast, we found that
399 the membrane localization of tGPH was strongly reduced in the larval fat body of GF
400 $Arc1^{E8}$ animals (Fig. 5F), indicative of reduced IIS pathway activation. Together these
401 data demonstrate that aside from the larval growth delay, wild type GF larvae do not have
402 phenotypes associated with reduced IIS signaling. However, when *Arc1* is also
403 eliminated, these animals exhibit many hallmarks of IIS deficiency. Likewise, *Arc1* mutant
404 *Acetobacter sp.* animals generally do not display evidence of IIS signaling defects. But
405 the starvation resistance of $Arc1^{E8}$ animals suggests that *Arc1* mutants may be sensitized
406 to reduced IIS signaling, which is exacerbated by GF rearing. Thus, *Acetobacter sp.* is
407 largely sufficient to promote IIS activity in *Arc1* mutants, suggesting a potential
408 mechanism by which *Acetobacter sp.* may promote organismal homeostasis in *Arc1*-
409 deficient hosts.

410 **DISCUSSION**

411 Here we reveal a novel and unexpected connection between the host gene *Arc1*
412 and the bacterial microbiota in *Drosophila*: we demonstrate that *Arc1* transcript levels are

413 responsive to the microbiota, and find that Arc1 functions to suppress metabolic and
414 fitness deficiencies induced by microbiota removal. *Arc1* exhibits microbiota-dependent
415 expression, as its transcript levels are elevated or repressed in a tissue-specific manner
416 in GF animals. Under our standard dietary conditions, GF rearing of wild type animals or
417 *Arc1* mutation in GNO animals independently induced no defects or only moderate
418 defects in host metabolism-related traits. However, when both the microbiota and *Arc1*
419 were lost, strong IIS-dependent metabolic phenotypes emerged. In animals lacking *Arc1*,
420 association with one specific *Acetobacter sp.* alone was sufficient to restore normal IIS
421 signaling and developmental rate. Our data suggest that *Acetobacter sp.* functions in this
422 capacity through multiple mechanisms, one of which involves dietary modification. Thus,
423 in GF *Arc1* mutants, we propose that host genotype and microbial condition converge on
424 the IIS pathway, leading to growth defects.

425 Role of Arc1 in insulin signaling in GF flies

426 We found that GF *Drosophila* lacking Arc1 exhibit phenotypes consistent with
427 reduced IIS activity. Connections between Arc1/Arc and IIS/insulin activity have been
428 considered previously. Arc expression can be strongly induced in cultured human
429 neuroblasts by treatment with exogenous insulin (Kremerskothen et al., 2002). Arc1 is
430 strongly expressed in one small cluster of large neurons in each lobe of both the larval
431 brain and the pars cerebralis region of the adult brain that are proximal to and partially
432 overlap with the insulin producing cells (IPCs; Mattaliano et al., 2007; Mosher et al., 2015).
433 Further, Mattaliano et al. (2007) found that selectively restoring Arc1 expression in the
434 IPCs was sufficient to revert the starvation resistance of *Arc1* mutants. Yet beyond
435 starvation resistance and the increased larval fat levels reported by Mosher et al. (2015),

436 loss of Arc1 resulted in no additional traits suggestive of reduced IIS signaling (Mattaliano
437 et al., 2007). However, our data now reveal a microbiota-dependent component of the
438 Arc1-IIS connection, as we primarily observed IIS-related phenotypes in *Arc1* mutants
439 grown under GF conditions. Further, Arc1 metabolic phenotypes are strongly influenced
440 by nutritional composition, as we found that the developmental rate of GF *Arc1*^{E8} animals
441 varied considerably on various dietary formulations.

442 The IIS pathway coordinates nutritional intake, metabolism, and growth in a
443 mechanistically conserved manner between *Drosophila* and vertebrates. The *Drosophila*
444 IIS pathway is functionally analogous to the combined roles of the mammalian insulin
445 pathway, which primarily regulates blood glucose levels, and the Insulin-like growth factor
446 (IGF) pathway, which coordinates organismal growth (Edgar, 2006). Our data suggest
447 that Arc1 is a regulator of IIS signaling, whose role is revealed by GF rearing. In addition,
448 Arc1 likely impacts metabolism- and growth-regulating cellular processes beyond IIS,
449 which may or may not contribute to the growth delay of GF *Arc1*^{E8} larvae. This is
450 evidenced by the increased wing size and enhanced starvation resistance of *Arc1*
451 mutants even in the presence of *Acetobacter sp.* (Figure 5D,E). Possible additional
452 pathways influenced by Arc1 include Hippo signaling, which controls organ growth (Zhao
453 et al., 2011), and ecdysone biosynthesis, which is nutrient responsive and regulates
454 developmental rate (Edgar, 2006).

455 How might Arc1 promote IIS-pathway activity? Mammalian Arc modulates synaptic
456 plasticity in part by enhancing the endocytosis, and consequently reducing the membrane
457 availability, of AMPA receptors (Chowdhury et al., 2006; DaSilva et al., 2016; Wall and
458 Corrêa, 2018). Although it has not been shown for Arc1, this molecular function suggests

459 that Arc proteins may have the ability to regulate the recycling of other receptors, like the
460 insulin receptor. An alternative mechanism is suggested by recent reports that *Drosophila*
461 Arc1 and mammalian Arc encode polypeptides that can self-assemble into mRNA-
462 containing capsid-like structures, which are released from mammalian and *Drosophila*
463 cell lines, and *Drosophila* neurons at the larval NMJ (neuromuscular junction) in
464 extracellular vesicles (EVs; Ashley et al., 2018; Erlendsson et al., 2019; Pastuzyn et al.,
465 2018). These Arc/Arc1 capsid-containing EVs are taken up by recipient cells in both
466 cultured mouse hippocampal neurons and at the NMJ, constituting a novel mechanism of
467 intercellular mRNA transfer (Ashley et al., 2018; Pastuzyn et al., 2018). The functional
468 significance of this mechanism in cell types and tissues outside the NMJ that may be
469 relevant here (e.g. IPC-adjacent neurons) has not been studied, but it is tempting to
470 speculate that Arc1-mediated mRNA transfer may play a role in Arc1's metabolic function.
471 Interestingly, Arc1 is broadly expressed; in addition to its expression in the brain
472 (Mattaliano et al., 2007; Mosher et al., 2015), Arc1 is also expressed in the prothoracic
473 gland (Mattaliano et al., 2007) and is transcriptionally enriched in the gut (FlyAtlas; Leader
474 et al., 2018), where we and others have observed microbiota-dependent transcript level
475 changes (Figure 1A; Bost et al., 2017; Dobson et al., 2016; Guo et al., 2014; Petkau et
476 al., 2017). Additionally, knockdown of the transcription factor Seven-up, which reduces
477 IIS activity, leads to strongly increased *Arc1* expression in the larval fat body (Musselman
478 et al., 2018). This implicates Arc1 in multiple organs that control energy homeostasis. We
479 predict that Arc1 capsid-dependent intercellular mRNA transport and/or endocytic based
480 receptor cycling might act at multiple nodes in the systemic inter-organ signaling
481 dynamics of IIS.

482 *Acetobacter sp.* support of *Arc1* mutant larval growth

483 While loss of *Arc1* significantly exacerbated the developmental delay of GF larvae,
484 we found that monoassociation with *Acetobacter sp.* was sufficient for *Arc1* mutants to
485 develop at the same rate as wild-type *Acetobacter sp.*-associated larvae (Figure 2B). The
486 reduced growth rate of GF *Drosophila* is one of the most consistent and reproducible
487 microbiota-dependent host traits documented in the literature. As such, the mechanistic
488 basis underlying microbial growth promotion has been investigated (reviewed in Strigini
489 and Leulier, 2016). Our study revealed both similarities and differences between
490 published mechanisms of bacterial impact on larval growth, and the ways *Acetobacter*
491 *sp.* promotes development in an *Arc1*-deficient host.

492 In laboratory *Drosophila* cultures, bacterial populations predominantly grow on the
493 diet substrate, and are ingested along with the food (Ludington and Ja, 2020). We found
494 that pre-conditioning the larval diet with *Acetobacter sp.* substantially accelerated GF
495 *Arc1* mutant development, suggesting that an interaction between *Acetobacter sp.* and
496 the larval diet is a key feature of this bacterial isolate's growth promoting activity (Figure
497 4D'). There is precedent for bacterial modification of the diet altering host metabolism and
498 growth in *Drosophila*. On nutritionally rich diets, *Acetobacter tropicalis* can prevent
499 excessive accumulation of triglycerides in adult flies by metabolizing glucose in the food
500 and reducing its availability to the host (Huang and Douglas, 2015). On nutritionally poor
501 diets, *L. plantarum* depletes the levels of sugars and branched-chain amino acids, and
502 increase the levels of glycolysis and fermentation products to promote larval growth
503 (Storelli et al., 2017). Because acetic acid bacteria frequently predominate the *Drosophila*
504 microbiota, the impacts of acetic acid on fly physiology and development have been

505 investigated (Kamareddine et al., 2018; Kim et al., 2017; Shin et al., 2011). As in Kim et
506 al. (2017), we found that acetic acid either increased or had no effect on the
507 developmental delay of wild-type or Arc1 mutant larvae (Figure 4C,C'), suggesting acetic
508 acid production by our *Acetobacter sp.* isolate likely has a minimal impact on *Arc1* mutant
509 development under our dietary conditions.

510 Importantly, our data reveal that association with a live population of *Acetobacter*
511 *sp.* is required for optimal growth rate promotion of *Arc1* mutants. This suggests that
512 additional mechanisms beyond dietary modification support larval development in the
513 absence of *Arc1*. In wild-type flies, commensal bacteria have been shown to promote
514 growth through mechanisms involving interactions between bacterial cell wall
515 components and gut cells. For example, D-alanylated teichoic acids in the *L. plantarum*
516 cell wall induce expression of intestinal peptidases, facilitating larval growth on protein-
517 poor diets (Consuegra et al., 2020; Matos et al., 2017). Further, the microbiota-responsive
518 immune deficiency (IMD) pathway, which is activated in enterocytes by DAP-type
519 peptidoglycan present in gram-negative and *Lactobacilli* cell walls, has been shown to
520 promote metabolic homeostasis and larval development (Davoodi et al., 2018;
521 Kamareddine et al., 2018).

522 Taken together, our data suggest that the full impact of live *Acetobacter sp.* on
523 *Arc1* mutant metabolism and development involves a combinatorial effect of dietary
524 modification and direct bacterial-host cell interactions. These two distinct modes of
525 microbiota activity are analogous to the modes by which the microbiota influence host
526 physiology in mammals. Bacterial breakdown of certain macro-nutrients (e.g. complex
527 polysaccharides) in the human gut has been linked to health and disease states

528 (Cockburn and Koropatkin, 2016). In contrast, other functions, such as immune cell
529 maturation and maintenance of gut epithelial architecture, appear to require bacterial cell-
530 derived antigens (Sekirov et al., 2010).
531
532 Proposed evolutionary conservation of Arc-microbiota-insulin connections
533 Our data raise the question of whether microbiota- and diet-responsive metabolism
534 regulation is a conserved function for Arc proteins. It has been shown that chronically
535 feeding mice a high fat diet (HFD), which induces insulin resistance and diabetic-like
536 phenotypes as well as cognitive impairments, leads to suppressed Arc expression in the
537 cerebral cortex and hippocampus (Chen et al., 2020; Mateos et al., 2009). Comparably,
538 flies reared on a HFD exhibited reduced memory formation and reduced Arc1 expression
539 in the head ($p<0.05$, 1.35 fold-change reduction; Rivera et al., 2019). In rodent models, it
540 is well established that HFD perturbs the composition of the gut microbiota in a manner
541 that can mediate diabetic and other disease phenotypes (Kim et al., 2012; Murphy et al.,
542 2015). Our data thus raise the intriguing and previously unconsidered possibility that Arc
543 function in the brain plays a role linking diet-induced gut dysbiosis to cognitive and
544 metabolic impairments.
545 **MATERIALS AND METHODS**
546 ***Drosophila* stocks and general rearing**
547 The following fly stocks were used in this study: w^{1118}, Canton-S, and Oregon-R are long-
548 term lab stocks originally from the Bloomington Drosophila Stock Center (BDSC), Top
549 Banana (kind gift from Dr. Michael Dickinson), *y[1] w[1]* (BDSC #1495), w^{1118}; $Arc1^{E8}$ (kind
550 gift from Dr. Vivian Budnik and Dr. Travis Thomson), *w[*]*; $Arc1^{esm113}$ (BDSC #37531),

551 *w[*]; Arc1*^{esm18} (BDSC #37530), *w[*];; P{w[+mC]=Arc1-GAL4.M}3* (BDSC #37533), *w*^{1118}*;*
552 *P{UAS-rpr.C}14* (BDSC #5824), *y[1]w[67c23];*
553 *P{w[+mC]y[+mDint2]=EPgy2}*Arc2*[EY21260]* (BDSC #22466), *w*^{118}*;; P{tGPH}4* (BDSC
554 #8164). Non-experimental fly stocks were maintained at 21-22°C. Our laboratory utilizes
555 a yeast-cornmeal-molasses diet of the following recipe (percentages are given as wt/vol
556 or vol/vol throughout Methods): 8.5% molasses (Domino Foods), 7% cornmeal (Prairie
557 Mills Products), 1.1% active dry yeast (Genesee Scientific), 0.86% gelidium agar
558 (MoorAgar). The diet is boiled for ~30-45 minutes, cooled to 60-65°C, supplemented with
559 0.27% propionic acid (Sigma) and 0.27% methylparaben (Sigma) and dispensed to
560 polypropylene vials. All experiments in this study utilized this diet formulation except those
561 presented in Figure 2, which were conducted on yeast-glucose diets. Yeast-glucose diets
562 consisted of the indicated proportions of active dry yeast (Genesee Scientific), dextrose
563 (Fisher Scientific), and gelidium agar (MoorAgar), and were prepared as described in
564 (Koyle et al., 2016). Diets were mixed, autoclaved, cooled to 60-65°C, supplemented with
565 propionic acid and methylparaben, and dispensed to autoclaved vials.

566 **Bacterial stocks**

567 The *Acetobacter sp.*, *Acetobacter pasteurianus*, *Lactobacillus plantarum*, and
568 *Lactobacillus brevis* stocks utilized in this study were all isolated from conventionally
569 reared Top Banana *Drosophila* cultures in our laboratory. Adult flies were surface
570 sterilized in 10% sodium hypochlorite and 70% ethanol, rinsed three times and
571 homogenized in phosphate buffered saline (PBS). Serial dilutions of fly homogenates
572 were plated on de Man, Rogosa, and Sharpe (MRS; Weber Scientific) and acetic acid-
573 ethanol (AE; 0.8% yeast extract, 1.5% peptone, 1% dextrose, 0.5% ethanol, 0.3% acetic

574 acid; Blum et al., 2013) agar plates. Colonies with distinct morphology were streaked for
575 isolation. Bacterial taxonomies were assigned by PCR amplification and sequencing of
576 the 16S rRNA gene using universal bacterial primers 8F (5'-
577 AGAGTTTGATCTGGCTCAG-3') and 1492R (5'-GGMTACCTTGTTACGACTT-3'; Eden
578 et al., 1991). Sequences were searched against the NCBI nr/nt database via blastn
579 (Altschul et al., 1990; Camacho et al., 2009; Morgulis et al., 2008) and taxonomies were
580 assigned based on >97% sequence homology. The 16S rRNA sequence for isolate A22
581 (*Acetobacter sp.*) bore >97% similarity with >five different *Acetobacter* species so we do
582 not assign a species-level taxonomic classification in this report.

583 **Generation of germ free and gnotobiotic fly cultures**

584 Germ free and gnotobiotic *Drosophila* cultures were generated according to established
585 methods (Koyle et al., 2016). Synchronous populations of embryos were collected on
586 apple juice agar plates. In a sterile biosafety cabinet, embryos were treated with 50%
587 sodium hypochlorite solution for two minutes to eliminate exogenous microbes and
588 remove the chorion. Embryos were then rinsed twice in 70% ethanol, twice in sterilized
589 milliQ water, and once in sterilized embryo wash (2% Triton X-100, 7% NaCl). Sterilized
590 embryos were then pipetted into autoclaved food vials to generate germ free cultures. To
591 generate gnotobiotic flies, overnight cultures of bacterial isolates were grown in MRS
592 broth (30°C with shaking for *Acetobacter* isolates and 37°C static for *Lactobacilli*). Sterile
593 food vials were inoculated with 40μL of overnight cultures (OD~1) immediately prior to
594 the addition of sterilized fly embryos. For polyassociated (GNO) flies, vials were
595 inoculated with 40μL of a 1:1:1:1 mixture of overnight cultures of the four indicated
596 bacteria.

597 All experimental *Drosophila* cultures were maintained in an insect incubator at 23°C, 70%
598 humidity, on a 12:12 light-dark cycle.
599 Larval and adult animals were confirmed as germ free or mono-/polyassociated by
600 homogenization in sterile PBS and plating on MRS and AE agar plates.
601 We did not maintain GF, GNO, or monoassociated flies over multiple generations; all
602 experiments utilized independently-derived germ free or gnotobiotic animals.

603 **Developmental timing measurements**

604 Synchronous populations of embryos were collected in a six-hour time window and
605 treated as described above to generate vials of defined microbial conditions. For
606 pupariation and eclosion rate analysis, the number of pupae formed or empty pupal
607 cases, respectively, were counted daily until 100% of the population had pupariated or
608 eclosed. The duration of larval development is strongly affected by crowding conditions
609 in the food (Klepsatel et al., 2018). Also, variable and unpredictable numbers of embryos
610 do not survive the bleach and ethanol washes employed to generate germ free and
611 gnotobiotic cultures (Koyle et al., 2016; Troha and Buchon, 2019; unpublished
612 observations). Therefore, vials containing fewer than ten and greater than forty animals
613 were omitted from analyses as either under- or over-crowded, respectively.
614 Larval instars were determined via mouth hook and/or posterior spiracle morphologies
615 (Oldroyd, 1951).
616 Larval length and pupal volume were measured from images using Fiji (Schindelin et al.,
617 2012). For pupal volume, length (l) and width (w) of each pupa were measured and
618 volume calculated as previously described (Layalle et al., 2008; Redhai et al., 2020):
619 $V=4/3\pi(l/2)(w/2)^2$.

620 **Larval feeding assays**

621 Larval feeding was assessed via dye consumption (Buhler et al., 2018; Libert et al., 2007;
622 Mosher et al., 2015; Shin et al., 2011). Stage-matched pre-wandering third instar larvae
623 were transferred to autoclaved fly food containing 1.8% FD&C Red #40 dye (Ward's
624 Science,) and allowed to feed for 3 hr at 23°C. Guts were then dissected from 20 larvae
625 in PBS and homogenized via bead beating in 1mL PBS. Homogenates were centrifuged
626 at 13,000 rpm for 1 minute to pellet debris and absorbance of the supernatant was
627 measured at 490nm with a Tecan Spark microplate reader. Weighed amounts of dyed
628 food were similarly homogenized in PBS and A_{490} readings collected to generate a
629 standard curve, which was used to calculate μg food consumed per larva.

630 Mouth hook contraction rates were assayed as described (Bhatt and Neckameyer, 2013).
631 Pre-wandering third instar larvae were transferred to apple juice plates coated with yeast
632 paste, given 30 seconds to acclimate, and contractions were counted manually for 30
633 seconds.

634 **Quantifying bacterial loads for monoassociated larvae**

635 Pre-wandering third instar larvae (8-10 animals per replicate) were removed from the food
636 and surface sterilized in 10% sodium hypochlorite for 1 minute. Larvae were then rinsed
637 three times in PBS and homogenized in 125μL PBS via bead beating for 30 seconds.
638 Homogenates were serially diluted in PBS and dilutions were plated on AE (for
639 *Acetobacter*) or MRS (for *Lactobacilli*) agar plates. Plates were incubated for 2-3 days at
640 either 30°C (AE) or 37°C (MRS), and resultant colonies were counted manually from
641 dilution plates bearing ~50-400 colonies. Bacterial loads were calculated as colony-

642 forming units (CFUs) per larva, as previously described (Koyle et al., 2016), and log
643 transformed for analysis.

644 **Dietary treatments**

645 *Acetobacter sp.*-conditioned diet

646 To generate *Acetobacter sp.*-conditioned fly food (Figure 4), autoclaved food vials were
647 inoculated with *Acetobacter sp.* overnight culture, as described above. Inoculated vials
648 were incubated for five days at 23°C. Vials were then incubated at 65°C for 3 hr to kill
649 bacteria. Sterility of the conditioned diet was confirmed by plating food and larval
650 homogenates on AE plates, which consistently yielded no bacterial growth. Heated diet
651 controls consisted of un-inoculated, autoclaved GF vials incubated at 65°C for 3 hr.

652 Heat-killed bacterial feeding

653 For experiments feeding GF larvae dead bacterial cells (Figure 4A), overnight cultures of
654 *Acetobacter sp.* were heat-killed at 65°C for 1 hr and autoclaved food vials were
655 inoculated with 40μL of heat-killed suspension prior to the addition of GF embryos. Vials
656 were further inoculated with 40μL heat-killed bacterial suspension daily until 100% of the
657 population had pupariated. Successful heat killing was confirmed for each daily inoculum
658 by plating undiluted heat-treated bacterial suspension on AE plates, and by plating larval
659 homogenates, which consistently yielded no bacterial growth.

660 Cell-free supernatant feeding

661 For *Acetobacter sp.* supernatant treatments (Figure 4B), overnight cultures of
662 *Acetobacter sp.* (3mL in MRS, grown as described above) were filtered twice through
663 0.22μm PVDF sterile membrane filters (Genesee Scientific). Autoclaved food vials were
664 inoculated with 40μL of filtered media immediately prior to addition of GF embryos, and

665 vials were further inoculated with 40μL of filtered media daily until 100% of the population
666 pupariated. Absence of live bacterial cells was confirmed by plating daily filtered media
667 on AE plates, and plating larval homogenates.

668 Acetic acid-supplemented diets

669 For acetic acid supplementation of GF larval fly cultures (Figure 4C, C'), fly food was
670 autoclaved and allowed to cool to ~50-60°C. Glacial acetic acid (Fisher Scientific) was
671 then added to defined volumes of food to the indicated final concentrations (vol/vol 0.1%
672 and 0.2%). For sodium acetate supplementation, solid sodium acetate (Sigma) was
673 added to autoclaved, cooled food to a final concentration of 50mM. Supplemented diets
674 were mixed thoroughly and dispensed to pre-autoclaved empty vials.

675 **Wing analysis**

676 Wings from adult females were dissected, mounted in Aqua-mount (Thermo Scientific),
677 and imaged with a QICAM-IR Fast 1394 camera (Q-Imaging) on a Zeiss Axioskop2 Plus
678 microscope. All measurements were collected using Fiji. Wing area was measured along
679 wing margin, excluding the hinge. For cell size analysis, trichome density was measured
680 with FijiWings2.3 software using the 150px trichome density feature (Dobens and
681 Dobens, 2013). Cell count per wing was determined by multiplying the cell density
682 measurement by the total area of the wing.

683 **Starvation resistance**

684 Five days post-eclosion, adult mated female flies were transferred to 1% agar-water vials,
685 8-10 flies per vial. Flies were transferred to fresh agar-water vials daily. Survival was
686 monitored daily until 100% of the population succumbed. The experiment was conducted

687 three times, ~50-120 animals per condition per replicate, and data were combined for
688 analysis.

689 **RT-qPCR**

690 Heads and guts (proventriculus to hindgut, excluding crop and malpighian tubules) from
691 5-7 days-post-eclosion adult male flies (8-10 animals per replicate) were dissected in ice
692 cold PBS and homogenized immediately in Trizol reagent (Thermo Fisher). RNA was
693 extracted using the Direct-zol RNA Miniprep kit (Zymo Research) exactly following the
694 manufacturer's protocol. High quality RNA ($A_{260nm/280nm}$ ~2; 500ng) was used as template
695 for cDNA synthesis using the qScript cDNA synthesis kit (QuantaBio). Product from cDNA
696 synthesis reactions was used for qPCR with the PerfeCTa SYBR Green Supermix
697 (QuantaBio) in an Applied Biosystems 7300 Real Time PCR System instrument. Data
698 were normalized to *Rpl32* and expression fold changes were calculated using the $2^{-\Delta\Delta Ct}$
699 method. Primers used in this study: *Rpl32* (5'- ATGCTAAGCTGTCGCACAAATG-3' and
700 5'- GTTCGATCCGTAACCGATGT-3'; Ponton et al., 2011), *Arc1* (5'-
701 CATCATCGAGCACAACAACC-3' and 5'-CTACTCCTCGTGCTGCTCCT-3'; Mosher et
702 al., 2015), *Arc2* (5'-CGTGGAGACGTATAAAGAGGTGG-3' and 5'-
703 GACCAGGTCTTGGCATCCC-3'; FlyPrimerBank (Hu et al., 2013)).

704 **Fluorescence imaging**

705 Fat bodies from pre-wandering third instar larvae were dissected in ice cold PBS and
706 fixed in 4% paraformaldehyde-PBS (Electron Microscopy Sciences) for 30 min at room
707 temperature. Fat bodies were rinsed three times in PBS and mounted in aqua-poly/mount
708 (Polysciences). Images were captured on a spinning disc microscope with a Celesta 1W
709 light engine (Lumencor), an X-Light V2 scan head (Crest Optics), and a Prime95B CMOS

710 camera (Photometrics) on a Zeiss Axiovert 200M using Metamorph software (Molecular
711 Devices).

712 **Statistical analysis**

713 Statistical tests were conducted and figures generated using R version 3.5.1 (R Core
714 Team, 2019). For development data, the average time to pupariation was calculated for
715 each vial from the number of individuals pupariating on each day until the entire
716 population completed larval development. These per-vial values from at minimum three
717 replicates were used for statistical analyses; full sample sizes and statistical test output
718 for all development experiments in this study are reported in Table S1. Throughout,
719 within-genotype comparisons among different treatments were conducted via one-way
720 analysis-of-variance (ANOVA), while comparisons among different genotypes and
721 treatments were conducted via two-way ANOVA, as indicated in the figure legends. Post-
722 hoc analysis among significantly different factors were conducted via Tukey test using the
723 "lsmeans" package (Lenth, 2016). RT-qPCR data were analyzed via Student's t-test.
724 Starvation survival data were compared via Cox proportional-hazards model analysis
725 using the "survival" package (Therneau, 2012). The threshold of statistical significance
726 was considered $p<0.05$.

727

728 **ACKNOWLEDGMENTS**

729 We thank members of the McCartney, Hiller, and Mitchell labs for helpful discussions
730 during the performance of the study. We thank Rory Eutsey (Hiller lab, Carnegie Mellon
731 University) for technical assistance with qPCR experiments. We would like to thank Dr.
732 John Woolford for providing feedback on the manuscript. The Top Banana fly stock was

a generous gift from Dr. Michael Dickinson's lab (CalTech). The *Arc1*^{E8} fly stock was a generous gift from Dr. Vivian Budnik and Dr. Travis Thomson (University of Massachusetts Medical School). We thank Bloomington Drosophila Stock Center for providing other fly stocks. We would like to thank the Woolford, Mitchell, and Hinman labs and the Molecular Biosensor and Imaging Center at Carnegie Mellon University for reagents and equipment.

Funding for this work was provided by a Charles E. Kaufman Foundation New Initiative Grant and a Carnegie Mellon University ProSEED/BrainHub seed grant to B.M.M. S.A.K. was supported by NSF Graduate Research Fellowship DGE 1252522 and DGE 1745016.

No competing interests declared.

REFERENCES

Alhowikan, A. M. (2016). Activity-Regulated Cytoskeleton-Associated Protein Dysfunction May Contribute to Memory Disorder and Earlier Detection of Autism Spectrum Disorders. *Med. Princ. Pract.* **25**, 350-354.

Altschul, S. F., Gish, W., Miller, W., Myers, E. W. and Lipman, D. J. (1990). Basic local alignment search tool. *J. Mol. Biol.* **215**, 403–10.

Ashley, J., Cordy, B., Lucia, D., Fradkin, L. G., Budnik, V. and Thomson, T. (2018). Retrovirus-like Gag Protein Arc1 Binds RNA and Traffics across Synaptic Boutons. *Cell* **172**, 262-274.e11.

Baker, K. D. and Thummel, C. S. (2007). Diabetic Larvae and Obese Flies-Emerging Studies of Metabolism in Drosophila. *Cell Metab.* **6**, 257–266.

Bhatt, P. K. and Neckameyer, W. S. (2013). Functional analysis of the larval feeding circuit in Drosophila. *J. Vis. Exp.* **81**, e51062.

Bi, R., Kong, L. L., Xu, M., Li, G. D., Zhang, D. F., Li, T., Fang, Y., Zhang, C., Zhang, B. and Yao, Y. G. (2018). The Arc Gene Confers Genetic Susceptibility to Alzheimer's Disease in Han Chinese. *Mol. Neurobiol.* **55** 1217-1226.

Bing, X. L., Gerlach, J., Loeb, G. and Buchon, N. (2018). Nutrient-dependent impact of microbes on Drosophila suzukii development. *MBio* **9**, e02199-17.

Blum, J. E., Fischer, C. N., Miles, J. and Handelsman, J. (2013). Frequent Replenishment Sustains the Beneficial Microbiome of Drosophila melanogaster. *MBio* **4**, e00860-13.

Bost, A., Franzenburg, S., Adair, K. L., Martinson, V. G., Loeb, G. and Douglas, A. E. (2017). How gut transcriptional function of *Drosophila melanogaster* varies with

767 the presence and composition of the gut microbiota. *Mol. Ecol.* **27**, 1848-1859.
768 **Britton, J. S., Lockwood, W. K., Li, L., Cohen, S. M. and Edgar, B. A.** (2002).
769 Drosophila ' s Insulin / PI3-Kinase Pathway Coordinates Cellular Metabolism with
770 Nutritional Conditions. *Dev Cell* **2**, 239–249.
771 **Broderick, N. A. and Lemaitre, B.** (2012). Gut-associated microbes of *Drosophila*
772 *melanogaster*. *Gut Microbes* **3**, 307–321.
773 **Brogiolo, W., Stocker, H., Ikeya, T., Rintelen, F., Fernandez, R. and Hafen, E.**
774 (2001). An evolutionarily conserved function of the Drosophila insulin receptor and
775 insulin-like peptides in growth control. *Curr Biol* **11**, 213–221.
776 **Broughton, S. J., Piper, M. D. W., Ikeya, T., Bass, T. M., Jacobson, J., Driege, Y.,**
777 **Martinez, P., Hafen, E., Withers, D. J., Leevers, S. J., et al.** (2005). Longer
778 lifespan , altered metabolism , and stress resistance in Drosophila from ablation of
779 cells making insulin-like ligands. *Proc Natl Acad Sci U S A* **102**, 3105–3110.
780 **Buhler, K., Clements, J., Winant, M., Bolckmans, L., Vulsteke, V. and Callaerts, P.**
781 (2018). Growth control through regulation of insulin signalling by nutrition-activated
782 steroid hormone in drosophila. *Dev.* **145**, dev165654.
783 **Camacho, C., Coulouris, G., Avagyan, V., Ma, N., Papadopoulos, J., Bealer, K. and**
784 **Madden, T. L.** (2009). BLAST+: Architecture and applications. *BMC Bioinformatics*
785 **10**, 421.
786 **Campillos, M., Doerks, T., Shah, P. K. and Bork, P.** (2006). Computational
787 characterization of multiple Gag-like human proteins. *Trends Genet.* **22**, 585-589.
788 **Carmichael, R. E. and Henley, J. M.** (2018). Transcriptional and post-translational
789 regulation of Arc in synaptic plasticity. *Semin. Cell Dev. Biol.* **77**, 3-9.
790 **Chaston, J., Newell, P. and Douglas, A.** (2014). Metagenome-wide association of
791 microbial determinants of host phenotype in Drosophila melanogaster. *MBio* **5**,
792 e01631-14.
793 **Chen, T. J., Chen, S. S., Wang, D. C. and Hung, H. S.** (2020). High-fat diet reduces
794 novelty-induced expression of activity-regulated cytoskeleton-associated protein. *J.*
795 *Cell. Physiol.* **235**, 1065–1075.
796 **Chowdhury, S., Shepherd, J. D., Okuno, H., Lyford, G., Petralia, R. S., Plath, N.,**
797 **Kuhl, D., Huganir, R. L. and Worley, P. F.** (2006). Arc/Arg3.1 Interacts with the
798 Endocytic Machinery to Regulate AMPA Receptor Trafficking. *Neuron*. **52**, 445-459.
799 **Cockburn, D. W. and Koropatkin, N. M.** (2016). Polysaccharide Degradation by the
800 Intestinal Microbiota and Its Influence on Human Health and Disease. *J. Mol. Biol.*
801 **428**, 3230–3252.
802 **Colombani, J., Raisin, S., Pantalacci, S., Radimerski, T., Montagne, J. and**
803 **Léopold, P.** (2003). A nutrient sensor mechanism controls Drosophila growth. *Cell*.
804 **114**, 739-749.
805 **Consuegra, J., Grenier, T., Baa-Puyoulet, P., Rahioui, I., Akherraz, H., Gervais, H.,**
806 **Parisot, N., Da Silva, P., Charles, H., Calevro, F., et al.** (2020). Drosophila-
807 associated bacteria differentially shape the nutritional requirements of their host
808 during juvenile growth. *PLoS Biol.* **18**, e3000681.
809 **Cottee, M. A., Letham, S. C., Young, G. R., Stoye, J. P. and Taylor, I. A.** (2019).
810 Structure of D. melanogaster ARC1 reveals a repurposed molecule with
811 characteristics of retroviral Gag. *Sci Adv* **6**, eaay6354.
812 **DaSilva, L. L. P., Wall, M. J., de Almeida, L. P., Wauters, S. C., Januário, Y. C.,**

Müller, J. and Corrêa, S. A. L. (2016). Activity-regulated cytoskeleton-associated protein controls AMPAR endocytosis through a direct interaction with clathrin-adaptor protein 2. *eNeuro*. **3**, ENEURO.0144-15.2016.

Davoodi, S., Galenza, A., Panteluk, A., Deshpande, R., Ferguson, M., Grewal, S. and Foley, E. (2018). The Immune Deficiency Pathway Regulates Metabolic Homeostasis in Drosophila. *J Immunol.* **202**, 2747-2759.

DiAngelo, J. R. and Birnbaum, M. J. (2009). Regulation of Fat Cell Mass by Insulin in Drosophila melanogaster. *Mol. Cell. Biol.* **29**, 6341-6352.

Dobens, A. C. and Dobens, L. L. (2013). Fijiwings: An open source toolkit for semiautomated morphometric analysis of insect wings. *G3 Genes, Genomes, Genet.* **3**, 1443-1449.

Dobson, A. J., Chaston, J. M. and Douglas, A. E. (2016). The Drosophila transcriptional network is structured by microbiota. *BMC Genomics* **17**, 975.

Douglas, A. E. (2018). The Drosophila model for microbiome research. *Lab Anim. (NY).* **47**, 157–164.

Eden, P. A. E., Schmidt, T. M., Blakemore, R. P. and Pace, N. R. (1991). Phylogenetic analysis of *Aquaspirillum magnetotacticum* using polymerase chain reaction-amplified 16S rRNA-specific DNA. *Int. J. Syst. Bacteriol.* **41**, 324–325.

Edgar, B. A. (2006). How flies get their size: genetics meets physiology. *Nat rev Genet.* **7**, 907–916.

Ekmekciu, I., von Klitzing, E., Fiebiger, U., Escher, U., Neumann, C., Bacher, P., Scheffold, A., Kühl, A. A., Bereswill, S. and Heimesaat, M. M. (2017). Immune responses to broad-spectrum antibiotic treatment and fecal microbiota transplantation in mice. *Front. Immunol.* **8**, 397.

Erkosar, B., Storelli, G., Mitchell, M., Bozonnet, L., Bozonnet, N. and Leulier, F. (2015). Pathogen Virulence Impedes Mutualist-Mediated Enhancement of Host Juvenile Growth via Inhibition of Protein Digestion. *Cell Host Microbe* **18**, 445–455.

Erkosar, B., Kolly, S., van der Meer, J. R. and Kawecki, T. J. (2017). Adaptation to Chronic Nutritional Stress Leads to Reduced Dependence on Microbiota in Drosophila melanogaster. *MBio* **8**, e01496-17.

Erlendsson, S., Morado, D. R., Shepherd, J. D. and Briggs, J. A. G. (2019). Structures of virus-like capsids formed by the drosophila neuronal Arc proteins. *Nat Neurosci.* **23**, 172-175.

Fromer, M., Pocklington, A. J., Kavanagh, D. H., Williams, H. J., Dwyer, S., Gormley, P., Georgieva, L., Rees, E., Palta, P., Ruderfer, D. M., et al. (2014). De novo mutations in schizophrenia implicate synaptic networks. *Nature*. **506**, 179-184.

Géminard, C., Rulifson, E. J. and Léopold, P. (2009). Remote Control of Insulin Secretion by Fat Cells in Drosophila. *Cell Metab.* **10**, 199–207.

Gilbert, L. I. (2008). Drosophila is an inclusive model for human diseases, growth and development. *Mol. Cell. Endocrinol.* **293**, 25-31.

Gilbert, J. A., Krajmalnik-Brown, R., Porazinska, D. L., Weiss, S. J. and Knight, R. (2013). Toward Effective Probiotics for Autism and Other Neurodevelopmental Disorders. *Cell* **155**, 1446–1448.

Guan, Z., Saraswati, S., Adolfsen, B. and Littleton, J. T. (2005). Genome-wide transcriptional changes associated with enhanced activity in the Drosophila

859 nervous system. *Neuron*. **48**, 91-107.
860 **Guo, L., Karpac, J., Tran, S. L. and Jasper, H.** (2014). PGRP-SC2 promotes gut
861 immune homeostasis to limit commensal dysb, iosis and extend lifespan. *Cell* **156**,
862 109–122.
863 **Guzowski, J. F., McNaughton, B. L., Barnes, C. A. and Worley, P. F.** (1999).
864 Environment-specific expression of the immediate-early gene Arc in hippocampal
865 neuronal ensembles. *Nat. Neurosci.* **2**, 1120-1124.
866 **Guzowski, J. F., Lyford, G. L., Stevenson, G. D., Houston, F. P., McGaugh, J. L.,**
867 **Worley, P. F. and Barnes, C. A.** (2000). Inhibition of activity-dependent arc protein
868 expression in the rat hippocampus impairs the maintenance of long-term
869 potentiation and the consolidation of long-term memory. *J. Neurosci.* **20**, 3993-
870 4001.
871 **Hayes, C. L., Dong, J., Galipeau, H. J., Jury, J., McCarville, J., Huang, X., Wang, X.**
872 **Y., Naidoo, A., Anbazhagan, A. N., Libertucci, J., et al.** (2018). Commensal
873 microbiota induces colonic barrier structure and functions that contribute to
874 homeostasis. *Sci. Rep.* **8**, 14184.
875 **Hu, Y., Sopko, R., Foos, M., Kelley, C., Flockhart, I., Ammeux, N., Wang, X.,**
876 **Perkins, L., Perrimon, N. and Mohr, S. E.** (2013). FlyPrimerBank: an online
877 database for Drosophila melanogaster gene expression analysis and knockdown
878 evaluation of RNAi reagents. *G3 (Bethesda).* **3**, 1607-1616.
879 **Huang, J.-H. and Douglas, A. E.** (2015). Consumption of dietary sugar by gut bacteria
880 determines *Drosophila* lipid content. *Biol. Lett.* **11**, 20150469.
881 **Jünger, M. A., Rintelen, F., Stocker, H., Wasserman, J. D., Végh, M., Radimerski,**
882 **T., Greenberg, M. E. and Hafen, E.** (2003). The Drosophila Forkhead transcription
883 factor FOXO mediates the reduction in cell number associated with reduced insulin
884 signaling. *J. Biol.* **2**, 20.
885 **Kamareddine, L., Robins, W. P., Berkey, C. D., Mekalanos, J. J. and Watnick, P. I.**
886 (2018). The Drosophila Immune Deficiency Pathway Modulates Enteroendocrine
887 Function and Host Metabolism. *Cell Metab.* **28**, 449-462.e5.
888 **Keebaugh, E. S., Yamada, R., Obadia, B., Ludington, W. B. and Ja, W. W.** (2018).
889 Microbial Quantity Impacts Drosophila Nutrition, Development, and Lifespan.
890 *iScience*. **4**, 247-259.
891 **Keith, S. A., Eutsey, R., Lee, H., Solomon, B., Oliver, S., Kingsford, C., Hiller, N. L.**
892 **and McCartney, B. M.** (2019). Identification of Microbiota-Induced Gene
893 Expression Changes in the Drosophila melanogaster Head. *bioRxiv*.
894 **Kim, K. A., Gu, W., Lee, I. A., Joh, E. H. and Kim, D. H.** (2012). High Fat Diet-Induced
895 Gut Microbiota Exacerbates Inflammation and Obesity in Mice via the TLR4
896 Signaling Pathway. *PLoS One*. **7**, e47713.
897 **Kim, G., Huang, J. H., McMullen, J. G., Newell, P. D. and Douglas, A. E.** (2017).
898 Physiological responses of insects to microbial fermentation products: insights from
899 the interactions between Drosophila and acetic acid. *J. Insect Physiol.* **106**, 13-19.
900 **Klepsatel, P., Procházka, E. and Gáliková, M.** (2018). Crowding of Drosophila larvae
901 affects lifespan and other life-history traits via reduced availability of dietary yeast.
902 *Exp. Gerontol.* **110**, 298-308.
903 **Koyle, M. L., Veloz, M., Judd, A. M., Wong, A. C.-N., Newell, P. D., Douglas, A. E.**
904 **and Chaston, J. M.** (2016). Rearing the Fruit Fly Drosophila melanogaster Under

905 Axenic and Gnotobiotic Conditions. *J. Vis. Exp.* **113**, 54219.
906 **Kramer, J. M., Davidge, J. T., Lockyer, J. M. and Staveley, B. E.** (2003). Expression
907 of Drosophila FOXO regulates growth and can phenocopy starvation. *BMC Dev.*
908 *Biol.* **3**, 5.
909 **Kremerskothen, J., Wendholt, D., Teber, I. and Barnekow, A.** (2002). Insulin-induced
910 expression of the activity-regulated cytoskeleton-associated gene (ARC) in human
911 neuroblastoma cells requires p21ras, mitogen-activated protein kinase/extracellular
912 regulated kinase and src tyrosine kinases but is protein kinase C-independ.
913 *Neurosci. Lett.* **321**, 153–156.
914 **Larsen, N., Vogensen, F. K., Van Den Berg, F. W. J., Nielsen, D. S., Andreasen, A.**
915 **S., Pedersen, B. K., Al-Soud, W. A., Sørensen, S. J., Hansen, L. H. and**
916 **Jakobsen, M.** (2010). Gut microbiota in human adults with type 2 diabetes differs
917 from non-diabetic adults. *PLoS One* **5**, e9085.
918 **Layalle, S., Arquier, N. and Léopold, P.** (2008). The TOR Pathway Couples Nutrition
919 and Developmental Timing in Drosophila. *Dev. Cell* **15**, 568–577.
920 **Leader, D. P., Krause, S. A., Pandit, A., Davies, S. A. and Dow, J. A. T.** (2018).
921 FlyAtlas 2: A new version of the Drosophila melanogaster expression atlas with
922 RNA-Seq, miRNA-Seq and sex-specific data. *Nucleic Acids Res.* **46**, D809–D815.
923 **Lenth, R. V.** (2016). Least-squares means: The R package lsmeans. *J. Stat. Softw.*
924 **Lesperance, D. N. A. and Broderick, N. A.** (2020). Meta-analysis of Diets Used in
925 Drosophila Microbiome Research and Introduction of the Drosophila Dietary
926 Composition Calculator (DDCC). *G3; Genes|Genomes|Genetics* g3.401235.2020.
927 **Libert, S., Zwiener, J., Chu, X., VanVoorhies, W., Roman, G. and Pletcher, S. D.**
928 (2007). Regulation of Drosophila life span by olfaction and food-derived odors.
929 *Science.* **315**, 1133-1137.
930 **Ludington, W. B. and Ja, W. W.** (2020). Drosophila as a model for the gut microbiome.
931 *PLoS Pathog.* **16**, e1008398.
932 **Luong, N., Davies, C. R., Wessells, R. J., Graham, S. M., King, M. T., Veech, R.,**
933 **Bodmer, R. and Oldham, S. M.** (2006). Activated FOXO-mediated insulin
934 resistance is blocked by reduction of TOR activity. *Cell Metab.* **4**, 133-142.
935 **Martino, M., Ma, D. and Leulier, F.** (2017). Microbial influence on Drosophila biology.
936 *Curr. Opin. Microbiol.* **38**, 165–170.
937 **Martino, M. E., Joncour, P., Leenay, R., Gervais, H., Shah, M., Hughes, S., Gillet,**
938 **B., Beisel, C. and Leulier, F.** (2018). Bacterial Adaptation to the Host's Diet Is a
939 Key Evolutionary Force Shaping Drosophila-Lactobacillus Symbiosis. *Cell Host*
940 *Microbe.* **24**, 109–119.
941 **Mateos, L., Akterin, S., Gil-Bea, F. J., Spulber, S., Rahman, A., Björkhem, I.,**
942 **Schultzberg, M., Flores-Morales, A. and Cedazo-Mínguez, A.** (2009). Activity-
943 regulated cytoskeleton-associated protein in rodent brain is down-regulated by high
944 fat diet in vivo and by 27-hydroxycholesterol in vitro. *Brain Pathol.* **19**, 69-80.
945 **Matos, R. C., Schwarzer, M., Gervais, H., Courtin, P., Joncour, P., Gillet, B., Ma, D.,**
946 **Bulteau, A.-L., Martino, M. E., Hughes, S., et al.** (2017). D-Alanylation of teichoic
947 acids contributes to Lactobacillus plantarum-mediated Drosophila growth during
948 chronic undernutrition. *Nat. Microbiol.* **2**, 1635-1647.
949 **Mattaliano, M. D., Montana, E. S., Parisky, K. M., Littleton, J. T. and Griffith, L. C.**
950 (2007). The Drosophila ARC homolog regulates behavioral responses to starvation.

Mol. Cell. Neurosci. **36**, 211–221.

McBrayer, Z., Ono, H., Shimell, M. J., Parvy, J. P., Beckstead, R. B., Warren, J. T., Thummel, C. S., Dauphin-Villemant, C., Gilbert, L. I. and O'Connor, M. B. (2007). Prothoracicotropic Hormone Regulates Developmental Timing and Body Size in Drosophila. *Dev. Cell*. **13**, 857-871.

McFall-Ngai, M., Hadfield, M. G., Bosch, T. C. G., Carey, H. V, Domazet-Lošo, T., Douglas, A. E., Dubilier, N., Eberl, G., Fukami, T., Gilbert, S. F., et al. (2013). Animals in a bacterial world, a new imperative for the life sciences. *Proc. Natl. Acad. Sci.* **110**, 3229–3236.

Mirth, C., Truman, J. W. and Riddiford, L. M. (2005). The role of the prothoracic gland in determining critical weight for metamorphosis in Drosophila melanogaster. *Curr. Biol.* **15**, 1769-1807.

Montana, E. S. and Littleton, J. T. (2006). Expression profiling of a hypercontraction-induced myopathy in Drosophila suggests a compensatory cytoskeletal remodeling response. *J. Biol. Chem.* **10**, 421.

Morgulis, A., Coulouris, G., Raytselis, Y., Madden, T. L., Agarwala, R. and Schäffer, A. A. (2008). Database indexing for production MegaBLAST searches. *Bioinformatics*, **24**, 1757–1764.

Mosher, J., Zhang, W., Blumhagen, R. Z., D'Alessandro, A., Nemkov, T., Hansen, K. C., Hesselberth, J. R. and Reis, T. (2015). Coordination between Drosophila Arc1 and a specific population of brain neurons regulates organismal fat. *Dev. Biol.* **405**, 280–290.

Murphy, E. A., Velazquez, K. T. and Herbert, K. M. (2015). Influence of high-fat diet on gut microbiota: A driving force for chronic disease risk. *Curr. Opin. Clin. Nutr. Metab. Care*. **18**, 515-520.

Musselman, L. P., Fink, J. L., Narzinski, K., Ramachandran, P. V., Hathiramani, S. S., Cagan, R. L. and Baranski, T. J. (2011). A high-sugar diet produces obesity and insulin resistance in wild-type Drosophila. *Dis. Model. Mech.* **4**, 842-849.

Musselman, L. P., Fink, J. L., Maier, E. J., Gatto, J. A., Brent, M. R. and Baranski, T. J. (2018). Seven-up is a novel regulator of insulin signaling. *Genetics*. **208**, 1643-1656.

Newell, P. D. and Douglas, A. E. (2014). Interspecies Interactions Determine the Impact of the Gut Microbiota on Nutrient Allocation in Drosophila melanogaster. *Appl. Environ. Microbiol.* **80**, 788–796.

Oldroyd, H. (1951). Biology of Drosophila. *Nature*.

Pastuzyn, E. D., Day, C. E., Kearns, R. B., Kyrke-Smith, M., Taibi, A. V., McCormick, J., Yoder, N., Belnap, D. M., Erlendsson, S., Morado, D. R., et al. (2018). The Neuronal Gene Arc Encodes a Repurposed Retrotransposon Gag Protein that Mediates Intercellular RNA Transfer. *Cell*. **172**, 275-288.e18.

Petkau, K., Ferguson, M., Guntermann, S. and Foley, E. (2017). Constitutive Immune Activity Promotes Tumorigenesis in Drosophila Intestinal Progenitor Cells. *Cell Rep.* **20**, 1784–1793.

Ponton, F., Chapuis, M. P., Pernice, M., Sword, G. A. and Simpson, S. J. (2011). Evaluation of potential reference genes for reverse transcription-qPCR studies of physiological responses in Drosophila melanogaster. *J. Insect Physiol.* **57**, 840–850.

997 **Redhai, S., Pilgrim, C., Gaspar, P., Giesen, L. van, Lopes, T., Riabinina, O.,**
998 **Grenier, T., Milona, A., Chanana, B., Swadling, J. B., et al.** (2020). An intestinal
999 zinc sensor regulates food intake and developmental growth. *Nature*. **580**, 263-268.
1000 **Rivera, O., McHan, L., Konadu, B., Patel, S., Sint Jago, S. and Talbert, M. E.** (2019).
1001 A high-fat diet impacts memory and gene expression of the head in mated female
1002 Drosophila melanogaster. *J. Comp. Physiol. B.* **189**, 179-198.
1003 **Robertson, F. W.** (1963). The ecological genetics of growth in Drosophila: 6. The
1004 genetic correlation between the duration of the larval period and body size in
1005 relation to larval diet. *Genet. Res.* **4**, 74-92.
1006 **Robertson, R. C., Manges, A. R., Finlay, B. B. and Prendergast, A. J.** (2019). The
1007 Human Microbiome and Child Growth – First 1000 Days and Beyond. *Trends*
1008 *Microbiol.* **27**, 131-147.
1009 **Rulifson, E. J., Kim, S. K. and Nusse, R.** (2002). Ablation of insulin-producing neurons
1010 in files: Growth and diabetic phenotypes. *Science.* **296**, 1118-1120.
1011 **Saichana, N., Matsushita, K., Adachi, O., Frébort, I. and Frebortova, J.** (2015).
1012 Acetic acid bacteria: A group of bacteria with versatile biotechnological
1013 applications. *Biotechnol. Adv.* **33**, 1260-1271.
1014 **Sampson, T. R. and Mazmanian, S. K.** (2015). Control of brain development, function,
1015 and behavior by the microbiome. *Cell Host Microbe* **17**, 565–576.
1016 **Sannino, D. R., Dobson, A. J., Edwards, K., Angert, E. R. and Buchon, N.** (2018).
1017 The Drosophila melanogaster Gut Microbiota Provisions Thiamine to Its Host. *MBio*
1018 **9**, e00155-18.
1019 **Schindelin, J., Arganda-Carreras, I., Frise, E., Kaynig, V., Longair, M., Pietzsch, T.,**
1020 **Preibisch, S., Rueden, C., Saalfeld, S., Schmid, B., et al.** (2012). Fiji: An open-
1021 source platform for biological-image analysis. *Nat. Methods*. **9**, 676-682.
1022 **Sekirov, I., Russell, S. L., Antunes, L. C. M. and Finlay, B. B.** (2010). Gut Microbiota
1023 in Health and Disease. *Physiol. Rev.* **90**, 859–904.
1024 **Shandilya, M. C. V. and Gautam, A.** (2020). Hippocampal Arc Induces Decay of
1025 Object Recognition Memory in Male Mice. *Neuroscience*. **431**, 193-204.
1026 **Shen, J., Obin, M. S. and Zhao, L.** (2013). The gut microbiota, obesity and insulin
1027 resistance. *Mol. Aspects Med.* **34**, 39–58.
1028 **Shepherd, J. D. and Bear, M. F.** (2011). New views of Arc, a master regulator of
1029 synaptic plasticity. *Nat. Neurosci.* **14**, 279–284.
1030 **Shin, S. C., Kim, S.-H., You, H., Kim, B., Kim, A. C., Lee, K.-A., Yoon, J.-H., Ryu, J.-**
1031 **H. and Lee, W.-J.** (2011). Drosophila Microbiome Modulates Host Developmental
1032 and Metabolic Homeostasis via Insulin Signaling. *Science.* **334**, 670–674.
1033 **Smith, K., McCoy, K. D. and Macpherson, A. J.** (2007). Use of axenic animals in
1034 studying the adaptation of mammals to their commensal intestinal microbiota.
1035 *Semin. Immunol.* **19**, 59-69.
1036 **Storelli, G., Defaye, A., Erkosar, B., Hols, P., Royet, J. and Leulier, F.** (2011).
1037 Lactobacillus plantarum promotes drosophila systemic growth by modulating
1038 hormonal signals through TOR-dependent nutrient sensing. *Cell Metab.* **14**, 403–
1039 414.
1040 **Storelli, G., Strigini, M., Grenier, T., Bozonnet, L., Schwarzer, M., Daniel, C., Matos,**
1041 **R. and Leulier, F.** (2017). Drosophila Perpetuates Nutritional Mutualism by
1042 Promoting the Fitness of Its Intestinal Symbiont Lactobacillus plantarum. *Cell*

Metab. **27**, 362-377.
Strigini, M. and Leulier, F. (2016). The role of the microbial environment in Drosophila post-embryonic development. *Dev. Comp. Immunol.* **64**, 39–52.
Team, R. C. (2019). R: A Language and Environment for Statistical Computing. *Vienna, Austria*.
Therneau, T. (2012). A Package for Survival Analysis in S. R package version. *Survival (Lond).*
Troha, K. and Buchon, N. (2019). Methods for the study of innate immunity in Drosophila melanogaster. *Wiley Interdiscip. Rev. Dev. Biol.* **8**, e344.
Verdu, J., Buratovicht, M. A., Wilder, E. L. and Birnbaum, M. J. (1999). Cell-autonomous regulation of cell and organ growth in Drosophila by Akt/PKB. *Nat. Cell Biol.* **1**, 500-506.
Wall, M. J. and Corrêa, S. A. L. (2018). The mechanistic link between Arc/Arg3.1 expression and AMPA receptor endocytosis. *Semin. Cell Dev. Biol.* **77**, 17-24.
Wong, A. C., Dobson, A. J. and Douglas, A. E. (2014). Gut microbiota dictates the metabolic response of Drosophila to diet. *J Exp Biol* **217**, 1894–1901.
Zhao, B., Tumaneng, K. and Guan, K. L. (2011). The Hippo pathway in organ size control, tissue regeneration and stem cell self-renewal. *Nat. Cell Biol.* **13**, 877-883.

FIGURES

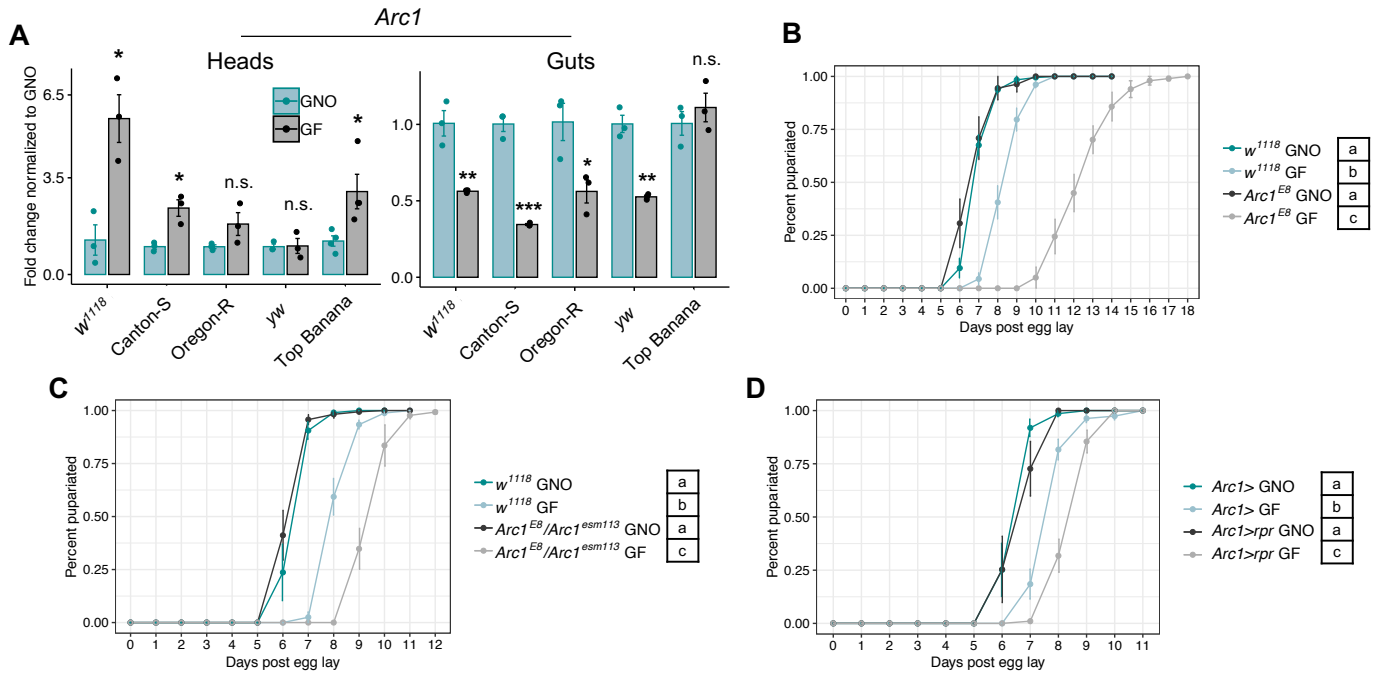

Figure 1. *Arc1* exhibits tissue-specific microbiota-dependent expression changes, and loss of *Arc1* exacerbates the developmental delay of GF larvae. A. RT-qPCR analysis of *Arc1* transcripts in heads and guts of 5-day-old adult male wild-type flies. Individual points represent normalized values for each replicate: n=3-4 per condition, 10 animals per replicate. Error bars represent standard error. * $p<0.05$, ** $p<0.01$, *** $p<0.001$, n.s. = not significant Student's t-test. **B,C.** Developmental time courses of GNO and GF wild-type/control *vs. Arc1* mutant animals, and **D.** larvae with *Arc1*-expressing cells ablated. *Arc1>*: *Arc1-Gal4* crossed to w^{1118} background control, *Arc1>rpr*: *Arc1-GAL4* crossed to *UAS-reaper*. Error bars represent standard error. Conditions sharing letters are not statistically different from one another, two-way ANOVA with Tukey's post-hoc test. For all developmental rate experiments, see Table S1 for full sample sizes and statistical results.

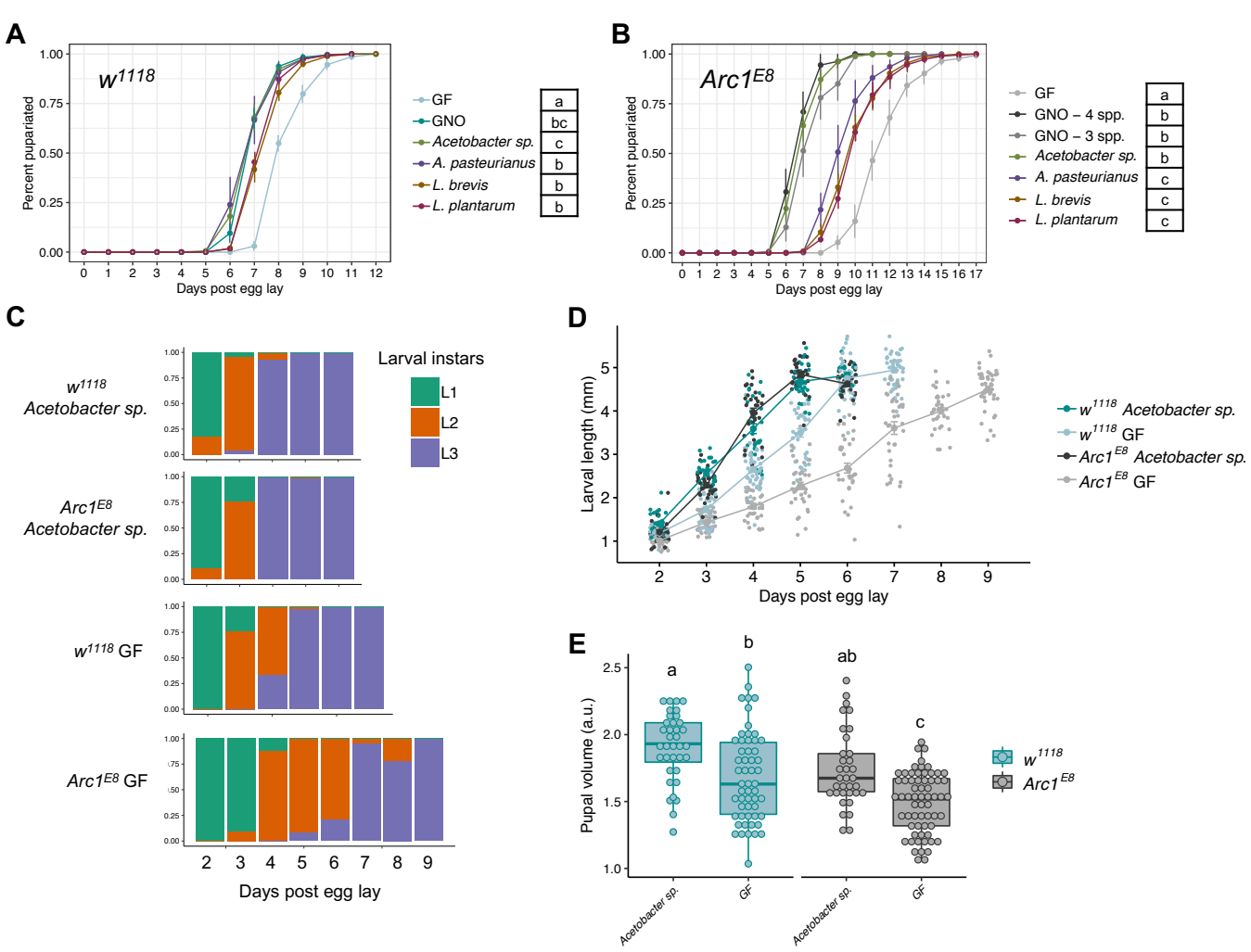

Figure 2. Monoassociation with *Acetobacter sp.* promotes development of *Arc1* mutant larvae. A, B. Time to pupariation for wild-type and *Arc1* mutant animals monoassociated with each of the four bacterial isolates comprising the GNO condition. GNO–3spp.: gnotobiotic community consisting of *A. pasteurianus*, *L. brevis*, and *L. plantarum.* Conditions sharing letters are not statistically different from one another, one-way ANOVA with Tukey's post-hoc test. **C.** Percentage of larvae in the indicated instar stage daily until 100% of the population reaches the pre-wandering or wandering third instar stage. Data represent pooled percentages from three biological replicates for

1135 each day, ~30-60 animals per day. **D.** Larval length for both genotypes and microbial
1136 conditions over time. Each data point represents an individual larva, three biological
1137 replicates, ~10-20 larvae per replicate. Error bars represent standard error. **E.** Pupal
1138 volume for each genotype and microbial condition. Each data point represents an
1139 individual pupa. Conditions that share a letter are not statistically different from one
1140 another, two-way ANOVA with Tukey's post-hoc test.
1141
1142
1143
1144
1145
1146
1147
1148
1149
1150
1151
1152
1153
1154
1155
1156
1157

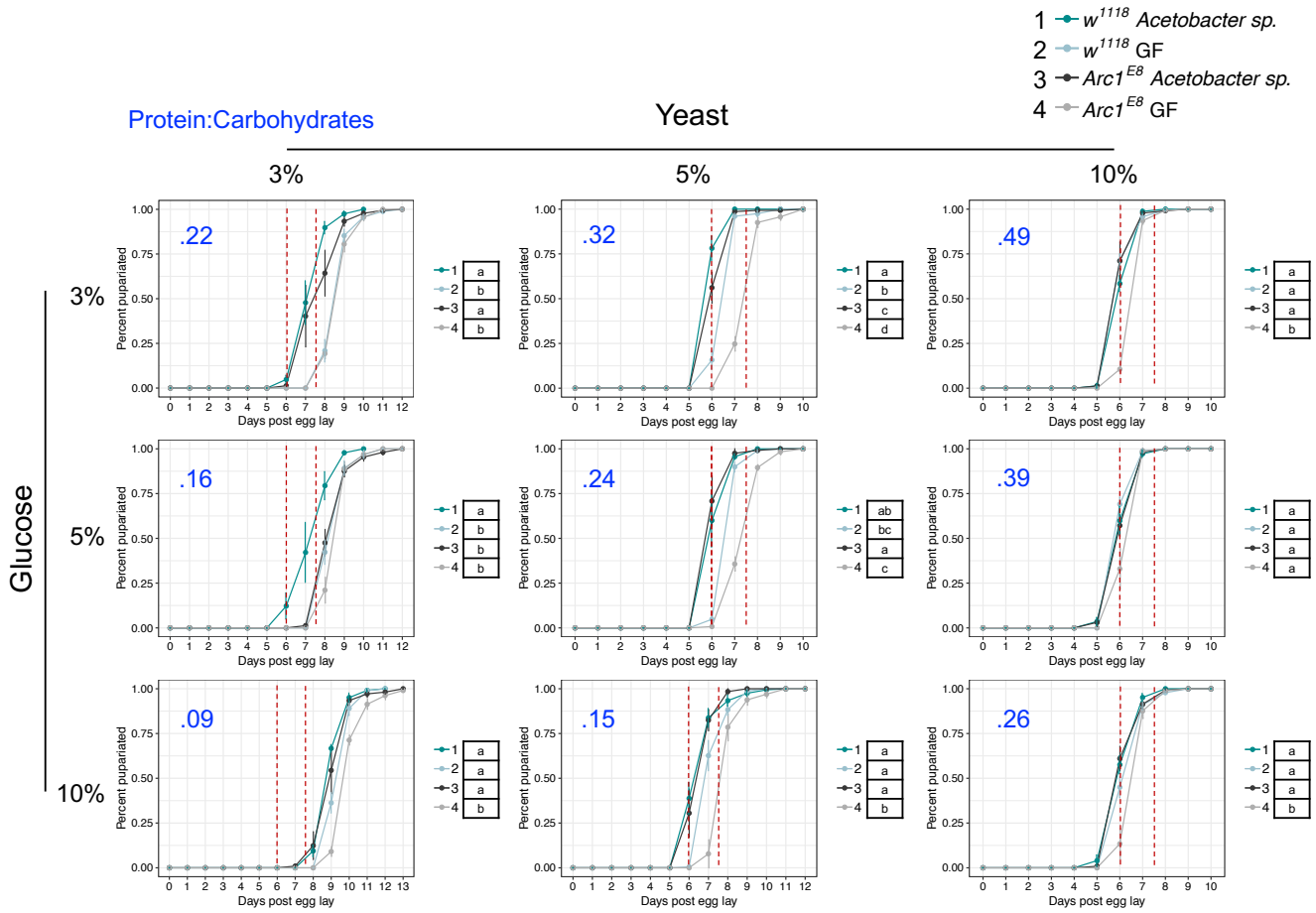

Figure 3. Host diet impacts microbial effects on wild-type and *Arc1* mutant developmental rate. Time to pupariation for wild-type and *Arc1*^{E8} *Acetobacter sp.*-associated and GF larvae reared on diets consisting of the indicated concentrations (weight/volume) of yeast and dextrose. Red dashed lines indicate the time to ~50% pupariation for *Arc1*^{E8} *Acetobacter sp.* and *Arc1*^{E8} GF animals on the 3% glucose-5% yeast diet as an arbitrary reference to facilitate visual comparisons among diets. Values in blue represent the protein:carbohydrate ratio for each diet as calculated with the Drosophila Diet Composition Calculator (Lesperance and Broderick, 2020). Conditions that share a letter are not statistically different from one another, two-way ANOVA with Tukey's post-hoc test.

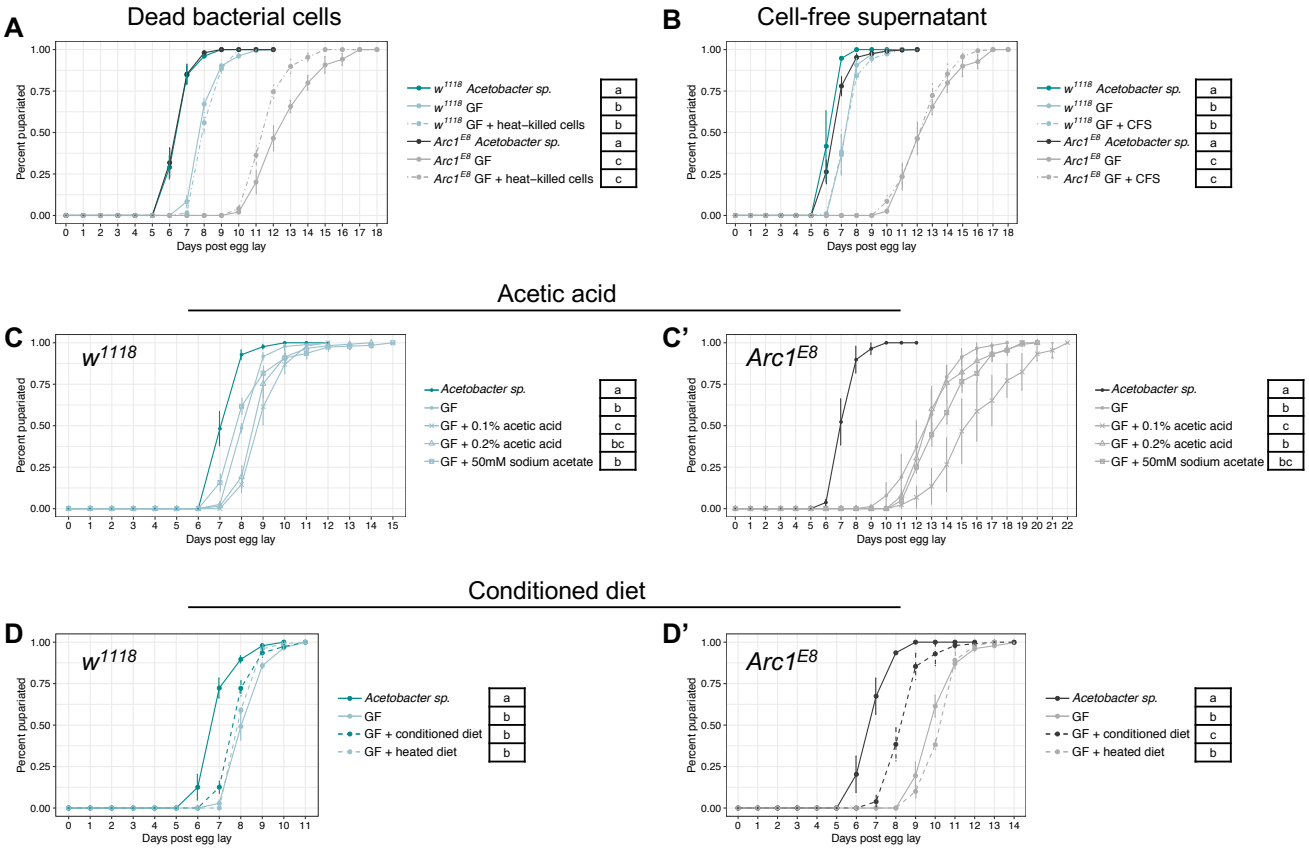

Figure 4. *Acetobacter sp.*-conditioned diet accelerates the development of *Arc1* mutants. A. Daily administration of heat-killed *Acetobacter sp.* planktonic culture has minimal effect on developmental rate of GF wild-type or *Arc1*^{E8} larvae. Two-way ANOVA with Tukey's post-hoc test. **B.** Daily administration of filtered supernatant from *Acetobacter sp.* planktonic culture has no effect on developmental rate of GF wild-type or *Arc1*^{E8} larvae. Two-way ANOVA with Tukey's post-hoc test. **C, C'.** Rearing GF wild-type and *Arc1* mutant larvae on diets containing acetic acid either further extends or has no effect on the larval developmental delay. Each panel analyzed by one-way ANOVA with Tukey's post-hoc test. **D, D'.** Rearing GF larvae on sterile diet that has been pre-conditioned with *Acetobacter sp.* for five days (GF + conditioned diet) has no effect on wild-type but partially restores developmental rate of *Arc1*^{E8} animals. GF + heated diet:

1204 GF larvae reared on GF diet heated under the same conditions used to kill *Acetobacter*
1205 *sp.* after pre-conditioning. Each panel analyzed by one-way ANOVA with Tukey's post-
1206 hoc test. Throughout, conditions that share a letter are not statistically different from one
1207 another.
1208
1209
1210
1211
1212
1213
1214
1215
1216
1217
1218
1219
1220
1221
1222
1223
1224
1225
1226

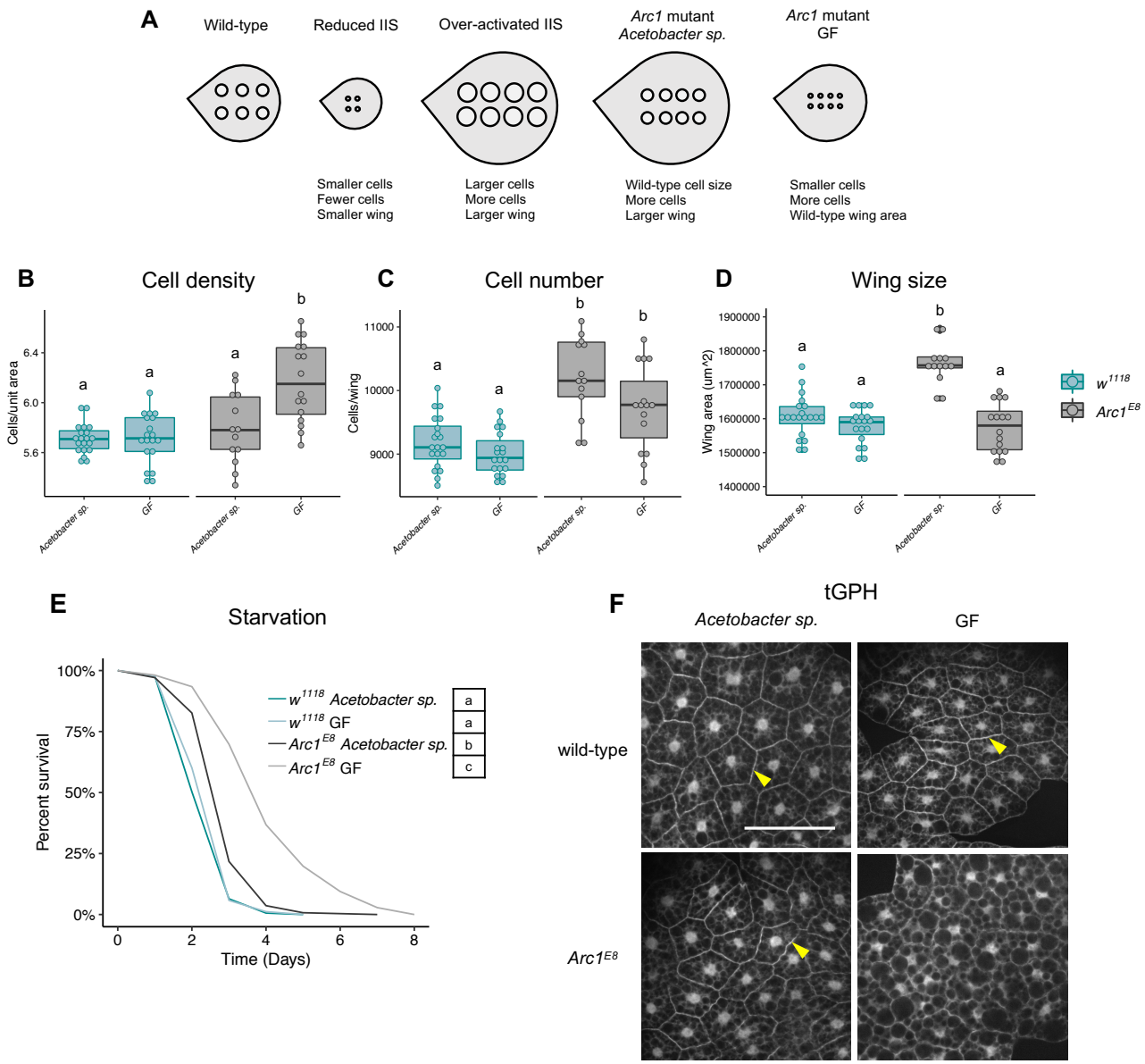

Figure 5. GF *Arc1* mutants exhibit phenotypes consistent with insulin signaling defects. A. Schematic representing impacts of insulin signaling manipulations and Arc1 mutation-microbial condition interactions on wing organ properties. **B-D.** Wing morphological parameters for wild-type and *Arc1*^{E8} females under *Acetobacter sp.*-associated and GF conditions. Each point represents an individual wing. Each panel analyzed by two-way ANOVA with Tukey's post-hoc test. **E.** Survival curves for adult

1250 female wild-type and *Arc1* mutant *Acetobacter sp.*-associated and GF animals
1251 transferred to starvation conditions 5-7 days post-eclosion. Data represent pooled
1252 results from three biological replicates, ~50-120 animals per condition per replicate.
1253 Statistical results represent Cox proportional-hazards model analysis. Conditions that
1254 share a letter are not statistically different from one another. **F.** Representative images
1255 showing GFP-tagged plextrin homology domain (tGPH) localization in the fat bodies of
1256 pre-wandering third instar larvae of the indicated genotypes and microbial conditions.
1257 Scale bar=100μm. Arrowheads indicate membrane-localized fluorescent signal.